

---

## Chemical Reactions in High-Speed Flows

J. F. Clarke

*Phil. Trans. R. Soc. Lond. A* 1991 **335**, 161-199

doi: 10.1098/rsta.1991.0042

---

### Email alerting service

Receive free email alerts when new articles cite this article - sign up in the box at the top right-hand corner of the article or click [here](#)

---

To subscribe to *Phil. Trans. R. Soc. Lond. A* go to:  
<http://rsta.royalsocietypublishing.org/subscriptions>

---

# Chemical reactions in high-speed flows

BY J. F. CLARKE

*Aerodynamics, Cranfield Institute of Technology, Bedford MK43 0AL, U.K.*

Hypersonic flows are distinguished by a capacity to provoke endothermic chemical reactions in their constituent molecules. Interactions of gas-flow and chemical activity also take place in combustible (exothermic) gas mixtures, such as may be found in propulsive devices. After a brief validation of the idea that chemically active flows can be adequately treated via Euler–Prandtl theory, the paper is devoted to a discussion of some particular features of chemically active very-high-speed Euler-inviscid flows. The treatment, which is fairly self-contained, brings out some of the similarities that exist between dissociative and combustible flows by emphasizing the central part played by shock-waves across which no chemical reaction takes place; in this way the treatment is novel and helps to point out the closer-than-usual links that exist between external and propulsive flows in the hypersonic environment. A new approach to the numerical computation of supersonic two-dimensional steady reacting flow fields is outlined, as is the potential role of large activation energy asymptotics in simple dissociating flows. Some new results and suggestions for the study of high-speed combustion bring the paper to a close.

## 1. Introduction

As a broad statement of fact it can be said that any predominantly steady flow of gas past a vehicle is characterized, when viewed by an observer attached to the vehicle, by the constancy of the sum of the kinetic and thermal energies of each element of the gas. The ratio of the former to the latter energy is proportional to the square of the local Mach number, so that a specifically hypersonic flow, by which one implies a very high value of Mach number in the free-stream ahead of the vehicle, is distinguished by its very large flow-energy levels. An observer travelling with the vehicle will always see the gas brought to rest at the surface by the ‘no slip’ action of viscosity, so that thermal energy levels in this crucial interfacial region between airflow and structure will tend to be exceptionally high unless action is taken to keep the surface cool. How to cope with the consequent rates of heat transfer from gas to vehicle was, and indeed still is, one of the most important problems that the designer of a hypersonic vehicle has to solve. Even supposing that one decides to make theoretical models of hypersonic flow by following the aerodynamicist’s classical route of first calculating an outer flow by using an inviscid Euler model of flow behaviour, and then correcting it to account for its failure to satisfy real physical requirements at the surface by making use of Prandtl’s boundary-layer theory, one will still encounter regions of relatively slow and therefore thermally very energetic flow in the inviscid Euler field. This is certainly true in the vicinity of stagnation points but it is also true, for example, over the whole undersurface of a vehicle during

*Phil. Trans. R. Soc. Lond. A* (1991) **335**, 161–199

*Printed in Great Britain*

161

atmospheric re-entry in view of the large angles of incidence that are often adopted to slow the vehicle down before too much thermal energy is transferred from the air to the vehicle itself.

It is these high levels of thermal energy that make many hypersonic flow fields different from their slower brethren, since they bring into play modes of internal molecular energy storage (usually vibrational modes) that are dormant under conditions of more modest temperature levels; this can ultimately lead to dissociation of polyatomic chemical species as a result of the violence of intermolecular encounters at such levels of thermal energy. In short, hypersonic flow is most readily distinguished from less-energetic supersonic flow by its association with significant changes in the internal structure of molecules within the flow; its dynamics become the dynamics of a chemically reacting or relaxing medium.

These things have been very well understood for many years now, since the first intensive phase of research into the aerodynamics of hypersonic flight in the 1950s and 1960s. Much of the information that was gleaned at the time found its way into books and monographs most of which are still available, if not from the publishers, then at least from the shelves of libraries (see, for example, Vincenti & Kruger 1965; Clarke & McChesney 1964, 1976 (referred to from now on as C & M); Wegener 1969, 1952): all of these books deal with some aspects of the influence of finite-rate reaction effects on the behaviour of compressible continuous media; Hayes & Probstein (1966) deal with hypersonic flows, mostly for ideal inert gases, but in many places with so-called real-gas effects in mind; Zel'dovich & Raizer (1966) describe a very wide range of physico-chemical effects on the behaviour of continua, and therefore have a great deal to say that is relevant to hypersonic aerodynamics, although their actual remit is very much broader than that. Much of this work, which was quite new to aerodynamicists at the time, starts with some fairly painstaking explanations of such fields as kinetic theory of gases, thermodynamics and statistical thermodynamics of gas mixtures, radiation, and the kinetics of chemical and internal-molecular energy change, relying on such texts as Hirschfelder *et al.* (1954), Chapman & Cowling (1970), and others for this kind of basic physics. Whilst obviously relying totally in its early stages on what was already available in the physical and chemical sciences at the time, the study of hypersonic flight did also inspire a good deal of research into many aspects of molecular physics and chemistry. This is especially exemplified by the rapid developments that subsequently took place in laser physics, particularly in the field of gas-dynamic lasers (see the review by Christiansen *et al.* (1975)).

Towards the middle of the 1960s, for a variety of reasons not all of which have turned out to be particularly good ones, the research effort into hypersonic flows went into a sharp decline, and teaching of the topic in the Universities effectively ceased. Of course significant research did continue in one or two countries but this is neither the time nor the place to try to write a history of efforts to learn about the science and technology of trans-atmospheric flight. However, it is important to reiterate the remark about the effect that the pause in hypersonic research had on teaching in the Universities since, as will appear shortly, this fact has an influence on the preparation of this particular article.

There is no doubt about the present re-invigoration of interest in hypersonic aerodynamics around the world. Inevitably there is a certain amount of rediscovery going on, particularly when it comes to the basics of the topic, and particularly in view of the virtual cessation of teaching over a period of several years. There is the natural necessity to rework some of the old ideas so that they should be compatible

with the use of the computer. For all practical purposes the latter arrived in the period between the times of intensive activity in hypersonics research, and has completely transformed both the expectations and the possibilities for theoretical prediction. Whilst undoubtedly essential to present and future progress, the computer does have some disadvantages when it comes to teaching a subject in which physics and chemistry have such a big part to play. There is, as ever, a need to study simple but educative situations so that the ultimate users of the power of the computer will have a clear view of what to expect from these extraordinary machines, and not simply be seduced by the scale of what they can do.

It has become apparent that integration of a hypersonic vehicle with its power plant holds out many possibilities for the future of hypersonic flight in planetary atmospheres. As a result there is a necessity to manage another kind of chemically active flow field to best advantage. The external flow around the vehicle is mostly involved with endothermic flows in which kinetic and/or thermal energy is used to break chemical bonds, whilst the propulsion problem demands consideration of exothermic chemical activity in which chemical energy is made available to the flow and not taken away from it. Although there are some radical differences in the way in which exothermic and endothermic systems behave, there are also some quite considerable points of similarity. This fact, coupled with statements in the previous paragraph, provides a general motivation for the account of chemically-active flows that is to follow.

Trans-atmospheric flight is distinguished not only by the speeds that are necessary to get a vehicle into orbit, but even more by the range of atmospheric densities that such a vehicle will encounter. At very high altitudes gas flow past the vehicle can no longer be treated as the flow of a continuum and it becomes necessary to formulate problems of flow past a hypersonic vehicle as problems in the kinetic theory of gases. It is therefore rather important to know that, in essence, most of the problems that involve direct interactions between chemical change and the gas flow itself are found in circumstances for which typical Reynolds numbers are high and the flow can be treated as the motion of a continuum; these facts are validated in §2.

Section 2 lays down a very few necessary facts from thermodynamics and the kinetics of chemical change. In view of the central part that these things play in the processes that form the main item for subsequent discussion, the brevity of this section, amounting almost to misrepresentation, must be open to criticism. As remarked above, the early texts on hypersonic flows devoted a considerable proportion of their space to accounts of these matters for the benefit of professional aerodynamicists, who had been astonishingly fortunate in having to deal with only the simplest models of ideal chemically inert substances to advance the science of aeronautics up to that time, at least as far as external flows were concerned. The space available for an account of such matters in an article of the present kind, that aims to concentrate on a few essential features of the flow of chemically active gases, is obviously a significant limiting factor. In mitigation, one can at least point to the existence of the old texts and also, now, to two new ones, by Anderson (1989) and Park (1990). Park in particular gives an extensive and up-to-date account of rate processes in real air, and includes a full discussion of the close interconnections between the excitation of vibrational modes of energy in the diatomic molecules that exist in high-temperature air and the rates of dissociation of these molecules into their separate atoms. It also deals with the important matters of ionization and radiation, neither of which will find a specific place in the present brief account of

very high speed flows, although some of what will be said here does extend fairly painlessly to take in the effects of these particular physical processes.

Consideration of flows themselves begins in §4 with statements, in an integral form, of the laws of conservation of mass, momentum, and energy, and of the conservation equations for individual chemical species, all according to the Euler model of fluid behaviour. This model is consistent with the findings in §2, and implies that the whole field of flow must ultimately be treated in the classical Euler–Prandtl fashion. Only the Euler formulation will be dealt with in this article; hypersonic boundary layers are to be described in another paper in the present collection, and one should also recollect the existence of the text by Dorrance (1962), which deals specifically with the effects of chemical activity on the character of high-speed shear layers.

Section 5 examines the kind of discontinuous behaviour that is admitted in solutions of the Euler equations, and identifies two distinct cases namely slip-surfaces, across which flow velocity and chemical composition can jump from one value to another, and shocks. The latter must obey two important relationships, one thermodynamical (the Hugoniot relation) and one fluid dynamical (the Rayleigh-line relation, in essence a rule for the behaviour of momentum); it transpires that the chemical composition must remain fixed, or frozen, as flow crosses the shock discontinuity.

The treatment in §5 allows for both endothermic and exothermic chemical action.

There is some discussion of the ways in which Hugoniot-curve–Rayleigh-line analysis can be extended to situations other than those for which the flow is chemically frozen, and also of the implications of these extensions for the treatment of curved shock waves.

The next section deals briefly with oblique shocks for the case of endothermic reaction downstream of the wave, and establishes some relations that will be useful in the work that is to follow.

Section 8 introduces the topic of continuous solutions of the Euler equations and describes some special results for the case of plane steady two-dimensional flow, employing the natural orthogonal curvilinear system of coordinates that uses streamlines as its basis. This system of coordinates has the advantage that many results appear in a very economical form and so are rather more easily understood; this applies particularly to the derivation of characteristic forms of the equations that govern behaviour in the continuous parts of the flow field. There can also be advantages for the construction of grids on which to make numerical calculations.

The Prandtl–Meyer expansion fan plays a very important part in studies of the two-dimensional steady flow of chemically inert gases. This particular flow phenomenon owes its simplicity to the fact that it is a similarity solution of the differential equations of motion and, accordingly, it is interesting to enquire whether such a similitude extends to the case of reacting flows. It is shown in §8 that there is no similarity solution when the differential equations of motion contain the ‘source’ terms that are necessary to describe the progress of chemical reactions. However, it is found that similitude is preserved for inert expansive flows in the natural coordinate system. A numerical computational method is therefore proposed that exploits the particular character of a natural coordinate system when making use of the operator-splitting methods that become necessary in the presence of finite-rate chemical reactions.

Section 9 takes up the matter of vorticity, since continuous creation of this fluid

property by the direct action of finite-rate chemical change is another feature of the reacting system that distinguishes it from inert flows. Amongst other things, a general expression is found in this section for the jump in vorticity experienced by fluid passing through any curved shock-wave that exists in a non-uniform reacting stream. Such shocks can be anticipated in hypersonic flows near deflected control surfaces, for example.

There is evidently some scope for the investigation of boundary-layer development beneath such vortical flows, particularly in the way that phenomena such as flow-separation and transition may be affected.

Section 10 examines some particular flows in order to illustrate in some detail how they interact with chemical activity. Consideration of a simple normal shock that initiates a single (endothermic) dissociation reaction shows how dissociative processes dominate and proceed very rapidly immediately downstream of the shock, to be followed by a much slower and protracted progress towards equilibrium as the recombination reaction begins to get under way. Of course there is nothing new about such results, but they are acquired here by a very economical and accurate approximate method adapted from recent work in combustion theory. Some of the lessons learnt in this first subsection of §10 are then applied to bring out basic features of flows through oblique shocks, and of flows in the neighbourhood of blunt bodies, where freezing of the dissociation reaction may be observed.

The last section in the paper turns to the rather different matter of combustion in high-speed flow, with an intention to understand some of the broad physical processes that will occur in propulsion devices that deposit chemical energy in supersonic streams. Starting from the concept of the Chapman–Jouguet detonation wave as one such physical process it is shown that the problem has close affinities with recent work on the unsteady evolution of detonations. As a consequence it can be seen that there are possibilities for combinations of shock-generated ignition and subsequent combustion, controlled to some degree by the flow itself, that do not involve detonation waves as such.

The paper attempts to give a general view of the way in which energy in the internal structure of molecules can influence a high-speed flow, and to do so in a way that emphasizes similarities between the treatment of endothermic and exothermic situations at least as much differences. Several new results will be found in the text, and some old results are derived or presented in new ways. It is hoped that there may be benefits from the unity of presentation which, in keeping with remarks made earlier in this Introduction, is generally didactic in character. Some lines of research are identified and not the least exciting of these is the effort that should go into developing the understanding of combustion in the high-speed flow environment.

## 2. Co-existence of continuum flow, finite-rate chemistry and high Reynolds number

The local Mach number  $M$  is an important parameter in any compressible flow because it is a measure of the kinetic energy of flow as a multiple of the gas's thermal energy. Strictly it is  $M^2$  that is proportional to this measure, since  $M$  is usually defined to be

$$M = u/a_f, \quad (2.1)$$

where  $u$  is local gas speed and  $a_f$  is local sound speed (strictly,  $a_f$  is the local *frozen* speed of sound; more will be said about this matter below). The association of  $a_f$  with

a local signal or sound speed is readily understandable when one remembers that  $a_f$  is an average thermal, or random, molecular speed ( $a_f^2$  is therefore indicative of the amount of thermal energy in the gas).

The kinematic viscosity of any gas, written as  $\nu$ , is related to  $a_f^2$  via

$$\nu = a_f^2 t_{\text{coll}} = a_f l, \quad (2.2)$$

where  $t_{\text{coll}}$  is an average time interval between collisions of pairs of molecules and

$$l \equiv a_f t_{\text{coll}} \quad (2.3)$$

is the local molecular mean free path, namely an average distance travelled by a molecule between successive collisions. Introducing a length scale  $L$  that typifies the situation under consideration,  $M$  in (2.1) can now be rewritten in the form

$$M = (uL/\nu)(\nu/La_f) = (uL/\nu)(l/L) \equiv (Re)(Kn), \quad (2.4)$$

where  $Re$  and  $Kn$  are the Reynolds number and Knudsen number respectively.

In any flow that is influenced by chemical reactions the ratio of local flow time  $L/u$  to local chemical time  $t_{\text{chem}}$  will evidently be significant. Reactions (e.g. dissociation) usually take place between pairs of molecules so that local chemical or relaxation times will be measured in multiples of  $t_{\text{coll}}$ ; i.e.

$$t_{\text{chem}} = t_{\text{coll}} \mathcal{R}. \quad (2.5)$$

The number  $\mathcal{R}$  is frequently very large and depends upon the energy of a molecular encounter; since the latter is most often signified by the value of absolute temperatures  $T$ ,  $\mathcal{R}$  is usually considered to be a function of  $T$  although, from what has been said above,  $a_f^2$  would be an equally good variable to use. The ratio  $L/ut_{\text{chem}}$  defines a local Damköhler number  $\mathcal{D}$ , namely

$$\mathcal{D} = L/ut_{\text{coll}} \mathcal{R} = (MKn\mathcal{R})^{-1}, \quad (2.6)$$

where the last result follows from (2.3) and the definitions of  $M$  and  $Kn$  in (2.1) and (2.4) respectively.

During re-entry of Earth's atmosphere by the U.S. Space-Shuttle Orbiter-Vehicle,  $Re$  lies in the range  $10^2$ – $10^7$ . With  $M$  of order 10, (2.4) implies that  $Kn$  is  $10^{-1}$ – $10^{-6}$  so that it is reasonable to treat re-entry as a problem in the dynamics of a continuum.

Furthermore, with  $\mathcal{R}$  of order  $10^4$  or greater,  $MKn\mathcal{R}$  is generally of order, or greater than, unity. Values of  $\mathcal{D} \leq 1$  imply that chemical times are comparable with, or larger than, flow times, with the consequence that finite-rate chemical and/or relaxational effects must be included in continuum models of re-entry flow behaviour.

Of course such statements as the ones just made are broad and indicative rather than precise and prescriptive. Rewriting (2.6) and (2.4) to give

$$\mathcal{D} = Re(M^2\mathcal{R})^{-1} \quad (2.7)$$

and remembering that  $Re$  and  $M$  can be purely local values, it is clear that wide local variations in  $\mathcal{D}$  are possible within the flow about any particular vehicle. The 'rate number'  $\mathcal{R}$  is invariably large, but local  $M$  values (behind a nearly normal shock-wave, for example) may be quite small, even in hypersonic flight.

Except at very large altitudes  $Re$  is large and it is therefore reasonable to treat the flow-field around a re-entry vehicle by the classical Euler–Prandtl, or boundary-layer, methods. The remainder of this article is confined to a discussion of the influence of finite-rate chemistry on Euler flows.

### 3. Thermodynamics and rate processes

The particular character of a gas or gas mixture, and its influence on dynamical behaviour, is found in its caloric and thermal equations of state. These can be written formally as

$$e = e(p, v, c_\alpha), \quad p = (v, T, c_\alpha), \quad h \equiv e + pv, \quad (3.1)$$

where  $e$ ,  $h$ ,  $p$ ,  $v$  and  $T$  are, respectively, intrinsic energy per unit mass, enthalpy per unit mass, pressure, specific volume ( $=1/\rho$  where  $\rho$  is density) and absolute translational temperature;  $c_\alpha$  stands for the set of mass fractions of chemical species  $\alpha$  ( $=1, 2, \dots, N$ ).

Strictly, of course, one should specify sufficient information to enable all of the internal-energy states of each molecule to be followed during the course of any flow. Simply for purposes of brevity in the present article, this is not done, and so some care must be taken with interpretation of results. Attention is drawn to the recent text by Park (1990), which goes into such matters in great detail, and also to C & M which uses a formulation of the basic equations of reacting gases that widens the meaning of chemical species to take in some prescription of internal-energy levels.

It is usually quite adequate to treat each pure chemical species in the mixture as thermally perfect; in other words its partial pressure  $p_\alpha$  will be given by

$$p_\alpha = \rho c_\alpha (\mathbb{R}/W_\alpha) T, \quad (3.2)$$

where  $\mathbb{R}$  is the universal gas constant and  $W_\alpha$  is the molecular mass of  $\alpha$ . The total pressure  $p$  is then just the sum of  $p_\alpha$  over all  $\alpha$ , with the result that

$$p = \rho (\mathbb{R}/W) T, \quad 1/W = \sum_{\alpha=1}^N c_\alpha / W_\alpha. \quad (3.3)$$

$W$  is the molecular mass of the mixture and depends directly on the set of  $c_\alpha$  values. As a result it can be seen that a mixture of thermally perfect gases does not behave like a thermally perfect gas when changes of chemical composition accompany changes in other thermodynamic quantities.

States of chemical equilibrium are prescribed for any pair of thermodynamic quantities, e.g.

$$c_\alpha = c_{\alpha\text{eq}}(p, v). \quad (3.4)$$

As a result, chemical disequilibrium implies that within the flow

$$c_\alpha \neq c_{\alpha\text{eq}}, \quad (3.5)$$

and it is in this way that a lack of equilibrium is recognized in hypersonic flow-fields. It is useful to note that, when complete chemical and thermal equilibrium prevails, using  $(p, v)$  or  $(p, T)$  or  $(\rho, T)$ , etc., as the pair of thermodynamic variables with which to calculate  $c_{\alpha\text{eq}}$  results in a set of identical values for these composition variables. If the  $(p, v)$  or  $(p, T)$ , etc., pairs are taken in a flow that is not in a state of chemical equilibrium each pair will be associated with different values of  $c_{\alpha\text{eq}}$ .

Despite its intrinsically arbitrary character it can often be useful to define local equilibrium values within a non-equilibrium flow. Naturally it is important to be consistent with any such definitions in the treatment of particular problems.

If chemical equilibrium is postulated to apply throughout a flow, (3.4) implies that



(3.1) can be shortened to read  $e = e(p, v)$ . This particular situation is sufficiently important to be worth acknowledging with the special notation

$$e = e_{\text{eq}}(p, v), \quad (3.6)$$

which can be continued with other variables as may be appropriate (e.g.  $p = p_{\text{eq}}(v, T)$  from (3.16)).

### Entropy

It is possible to make a lot of progress with the solution of problems in gas-dynamics without even raising the matter of entropy. However, it is occasionally convenient or even necessary to introduce this variable; writing  $s$  for the specific entropy of a mixture of  $N$  chemical species the Gibbs relation can be presented in the form

$$T ds = dh - v dp - \sum_{\alpha=1}^N \mu_{\alpha} dc_{\alpha} \quad (3.7)$$

(cf. §1.11, 13–15 in C & M), where the  $\mu_{\alpha}$  quantities are partial specific Gibbs, or chemical, potentials. That is to say, with Gibbs potential for the mixture defined by  $g = h - Ts$ ,

$$\mu_{\alpha} = (\partial g / \partial c_{\alpha})_{p, T, c_{\beta}} = h_{\alpha} - Ts_{\alpha}, \quad (3.8)$$

where  $h_{\alpha}, s_{\alpha}$  are the partial enthalpy and entropy of species  $\alpha$  respectively (note that the condition of fixed pressure  $p$  must be taken to mean that each separate partial pressure  $p_{\alpha}$  is fixed; subscript  $c_{\beta}$  implies that all mass fractions except  $c_{\alpha}$  are fixed during the differentiation). Both  $h_{\alpha}$  and  $s_{\alpha}$  are made up from sums of translational and molecular-internal energies and entropies.

If changes in the  $c_{\alpha}$ -quantities take place sufficiently quickly relative to changes in other flow variables it is often assumed that they do so via states of local equilibrium. Naturally this does not mean that the  $dc_{\alpha}$  vanish. Instead, certain combinations of chemical potentials, that are associated with particular chemical reactions in the system, do go to zero. In such circumstances it can be shown (cf. C & M, §1.14) that (3.7) reduces to

$$T ds = dh - v dp \quad (3.9)$$

when equilibrium conditions prevail. Of course (3.7) also takes this identical form when the flow is frozen, since each and every  $dc_{\alpha}$  is equal to zero in that case; one must remember that differential increments, such as  $ds$  and  $dh$ , have very different meanings in the two limiting situations of frozen and equilibrium flows.

### Sound speeds

Among the most important derived thermodynamic quantities are the speeds of sound-propagation through the gas mixture. It is necessary to use the plural here in view of the fact that sound speeds depend upon certain partial derivatives of enthalpy and/or intrinsic energy and it is therefore essential to state, not only which thermodynamic variable is held constant and which is to change, but also what is to be done with each of the  $c_{\alpha}$  terms during the processes of differentiation.

Two limiting sound speeds are of most significance:

- (i) frozen sound speed  $a_{\text{f}}$ , for which all  $c_{\alpha}$  are fixed;
- (ii) equilibrium sound speed  $a_{\text{e}}$ , for which all  $c_{\alpha}$  follow their local equilibrium values;  $a_{\text{e}}$  is only unambiguous when the field through which the sound waves propagate is in a true state of chemical and thermal equilibrium.

The study of sound-wave propagation through a reacting or relaxing atmosphere

is not a trivial task, although many results are now well-established. A very early study of propagation through a dissociating gas was undertaken by Einstein (1920) and since then the matter has been taken up, re-worked, and extended in various ways, by a large number of people. For present purposes it must suffice to list a few directly relevant facts (C & M can be consulted for details and explanations).

Frozen sound speed is defined by the relation

$$a_f^2 = -(\partial h / \partial \rho)_{p, c_\alpha} / (\partial e / \partial p)_{p, c_\alpha} \quad (3.10)$$

Equilibrium sound speed is defined by

$$a_e^2 = -(\partial h_{\text{eq}} / \partial \rho)_p / (\partial e_{\text{eq}} / \partial p)_p \quad (3.11)$$

and it must always be the case that

$$(a_f^2)_{\text{eq}} > a_e^2 \quad (3.12)$$

where  $( )_{\text{eq}}$  implies that  $a_f^2$  is to be evaluated at the same equilibrium state as the one that applies to  $a_e^2$ .

Sound propagation in a reacting gas is dispersive and dissipative; harmonic waves which have real frequencies have phase speeds that approach  $a_f$  as their frequency increases without bound, and  $a_e$  as their frequency diminishes to zero. High-frequency waves are relatively strongly damped, low-frequency waves are relatively lightly damped.

In view of the near-equilibrium character of low-frequency waves it is possible to represent the damping effect of reaction or relaxation in an approximate way by the addition of an equivalent bulk viscosity to the shear-viscosity term that appears in the 'diffusivity' of sound (Lighthill 1956). The equivalent bulk viscosity idea is of very restricted validity (C & M, §1.15 and ch. 2).

### Reaction rates

The one feature that makes the flow of gases at high speeds and temperatures different from behaviour under more modest conditions is the creation or destruction within the flow of chemical species. The consequent movement of energy into and out of the energies of chemical bonds, or the internal structures of molecules, must exert direct influence on the flow since such energy can only be drawn from thermal or kinetic energy of the flow itself.

A proper understanding of the form and character of chemical reaction rates is therefore crucial. The study of chemical kinetics is a large discipline in its own right and any attempt to even summarize it here would be absurd. An important recent text that gives much up-to-date information on the kinetics of chemical and internal molecular change as it affects the behaviour of air is the book by Park (1990), although some information on the matter is available in all of the texts quoted in the Introduction. For present purposes a grossly simple caricature of a chemical rate expression must suffice.

First, one must acknowledge that chemical activity in almost all hypersonic flows proceeds as a result of molecular collisions. Expressions for the rate of production of a chemical species must therefore contain a term that signifies the probability of molecular encounters, and must therefore contain products and powers of concentrations of the species (usually given in terms of mass fractions  $c_\alpha$ ). As explained in §2, the rate at which such molecular encounters produce new species must be some multiple, usually a very large one, of the average time-interval

between molecular collisions. As a result the rate of production of a chemical species  $\alpha$ , say, in units of mass per unit volume per unit time, can be written as  $K_\alpha$ , where

$$K_\alpha = (\rho/t_{\text{chem}}) \mathbb{P}(c_\alpha, \rho, T). \quad (3.13)$$

Here  $\mathbb{P}$  is the collision probability factor, which does usually depend upon density and temperature as well as on the  $c_\alpha$  quantities, whilst  $t_{\text{chem}}$  is a chemical time (cf. §2) that will also usually depend upon  $\rho$  and  $T$ .

The key features of (3.13) are the algebraic (not differential) character of the numerator  $\rho\mathbb{P}$  and the existence of time  $t_{\text{chem}}$  in the denominator.

Chemical equilibrium is achieved when  $\mathbb{P} = 0$ , and it is evident that any non-zero value for  $\mathbb{P}$  is expressive of the degree of departure of actual local  $c_\alpha$  values from equilibrium values based on local  $\rho, T$  conditions.

#### 4. Integral form of the conservation equations

If, as is suggested in §2, all transport effects are neglected and the flow is steady, the integral forms of the conservation laws for mass, momentum, and energy are

$$\int_{\mathcal{A}} \rho \mathbf{u} \cdot \mathbf{n} \, d\mathcal{A} = 0, \quad (4.1)$$

$$\int_{\mathcal{A}} \{p\mathbf{n} + \rho \mathbf{u} \cdot \mathbf{nu}\} \, d\mathcal{A} = 0. \quad (4.2)$$

$$\int_{\mathcal{A}} (e + pv + \frac{1}{2}\mathbf{u} \cdot \mathbf{u}) \rho \mathbf{u} \cdot \mathbf{n} \, d\mathcal{A} = 0, \quad (4.3)$$

where  $\rho$ ,  $p$ ,  $e$  and  $\mathbf{u}$  are density, pressure, specific intrinsic energy and flow velocity vector respectively. The integrations are taken over a fixed surface  $\mathcal{A}$ , that surrounds a finite volume  $\mathcal{V}$  of the flow field ( $\mathbf{n}$  is the unit vector normal to  $\mathcal{A}$  that points out of  $\mathcal{V}$ ).

Since  $e$  depends upon both the chemical composition of the gas mixture and on the energy content of the various modes of motion within the internal structures of the molecules it is necessary to write down conservation laws for these variables too. Thus, with  $c_\alpha$  denoting the mass fraction of a species  $\alpha$ , it follows that one must make

$$\int_{\mathcal{A}} \rho c_\alpha \mathbf{u} \cdot \mathbf{n} \, d\mathcal{A} = \int_{\mathcal{V}} K_\alpha \, d\mathcal{V}, \quad \alpha = 1, 2, \dots, N, \quad (4.4)$$

where  $K_\alpha$  is the local rate of production of species  $\alpha$  in units of mass per unit volume per unit time as a result of chemical reactions;  $K_\alpha$  is integrated over the whole volume  $\mathcal{V}$  on the right-hand side of (4.4).

#### 5. Discontinuous behaviour and the requirements of conservation

The set of integral (Euler) conservation laws in §4 admits the possibility of discontinuous solutions for some of the flow variables. Assuming that discontinuities occur across a surface  $S: S(\mathbf{x}) = 0$  they must appear in one of two forms, depending on whether  $\mathbf{u} \cdot \mathbf{v}$  is zero or not zero, where

$$\mathbf{v} = \nabla S / |\nabla S| \quad (5.1)$$

is the unit vector normal to the surface  $S$ .

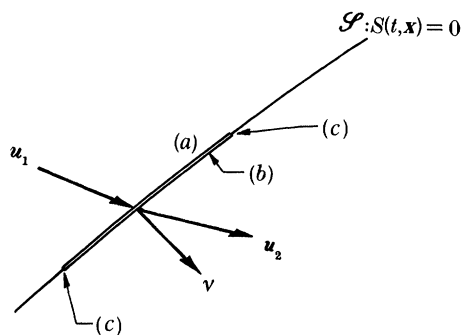


Figure 1. Conditions at a discontinuity-surface  $\mathcal{S}$ .  $\mathcal{A}_1$  (a),  $\mathcal{A}_2$  (b) and  $\mathcal{A}_e$  (c) make up the surface  $\mathcal{A}$  that surrounds volume  $\mathcal{V}$  (cf. §4);  $\mathcal{V} \rightarrow 0$  in the present situation.

When the normal component of velocity

$$u_n \equiv \mathbf{u} \cdot \mathbf{v} \quad (5.2)$$

is zero  $S$  is a slip or contact surface  $\mathcal{C}$ ; all physical variables in §4 may experience jumps across  $\mathcal{C}$  except, trivially,  $u_n$  itself and, from (4.2), the pressure  $p$ . The fact that tangential components of velocity

$$\mathbf{u}_t = \mathbf{u} - u_n \mathbf{v} \quad (5.3)$$

may be different on either side of  $\mathcal{C}$  accounts for the name ‘slip surface’, but it is potentially at least as interesting to observe that chemical composition may suffer discontinuous change across  $\mathcal{C}$ , which may therefore separate regions of different chemical composition.

When  $u_n \neq 0$  the character of  $S$  is quite different from  $\mathcal{C}$ ; the new discontinuity surface will be called  $\mathcal{S}$  from now on. Figure 1 is a sketch of the general situation, with gas-velocity components in the plane of the paper ahead and downstream of a discontinuity surface.

If subscript 2(1) identifies a value downstream (upstream) of  $\mathcal{S}$  it is useful to define  $[f]$ :

$$[f] \equiv f_2 - f_1, \quad (5.4)$$

since the jump relations that derive from (4.1)–(4.3) can then be written as

$$[\rho u_n] = 0 \Rightarrow \rho_1 u_{n1} = \rho_2 u_{n2} = m \neq 0, \quad (5.5)$$

$$[u_t] = 0, \quad (5.6)$$

$$[p + \rho u_n^2] = 0, \quad (5.7)$$

$$[h + \frac{1}{2}u_n^2] = 0. \quad (5.8)$$

These results emerge quite simply from (4.1)–(4.3) by letting the volume  $\mathcal{V} \rightarrow 0$ ; the surface  $\mathcal{A}$  then shrinks down to enclose  $\mathcal{S}$ , as indicated in figure 1. The quantity  $m$  is the mass-flux through  $\mathcal{S}$ , and is defined in (5.5) for later convenience.

On physical grounds one expects to find that the rate terms  $K_\alpha$  are bounded, with the consequence, from (4.4), (4.5) and (5.5), that  $\mathcal{V} \rightarrow 0$  demands

$$[c_\alpha] = 0. \quad (5.9)$$

The  $\mathcal{S}$ -like discontinuities that are admissible as solutions of the Euler equations are therefore fundamentally of a kind that can be designated ‘frozen’, since chemical and/or internal-molecular changes are not allowed to take place across them. As such these  $\mathcal{S}$  waves are formally identical with the shock discontinuities that propagate in Euler models of chemically inert and non-relaxing gases.

It is well known (see, for example, Whitham 1974, ch. 1) that the shock discontinuity is the best that the Euler equations can do to describe the real physical system in which nonlinear effects in wave propagation compete locally with the diffusive influences of (primarily) viscosity and thermal conduction (Lighthill 1956). The latter is a ‘Navier–Stokes’ explanation of shock-structure in a continuum, and shows that shock thickness is measured on a scale of molecular mean free path  $l$  (cf. (2.3)). As a shock strength increases the Navier–Stokes predictions of shock structure become increasingly inaccurate in the shock’s upstream regions and it then becomes necessary to resort to kinetic theory for accurate results (see, for example, Bird 1976). The total change from upstream-inflow to downstream-outflow across the shock-wave is still described by the jump relations (5.5)–(5.8) provided that the local radius of curvature of the shock is very much greater than its ‘Navier–Stokes’ or ‘kinetic-theory’ thickness (roughly  $l$ ). For all practical purposes this proviso is never violated in any flow for which Euler–Prandtl theory is valid.

The jump conditions in this section are exact in the context of both inert and chemically active Euler flows. The next section translates the jump conditions into some particularly useful forms, and then extends their applicability somewhat by considering systems for which the smallest radius of curvature of surface  $\mathcal{S}$  is very large compared with a chemical or relaxation length, such as  $u_n t_{\text{chem}}$  (cf. §2).

## 6. Hugoniot-curve and Rayleigh-line relations

The jump relations in (5.5)–(5.8) can be used to show that

$$\mathcal{L}: [p] + m^2[v] = 0, \quad (6.1)$$

$$\mathcal{H}_f: 2[h] - (v_2 + v_1)[p] = 2[e] + (p_2 + p_1)[v] = 0. \quad (6.2)$$

The Rayleigh line  $\mathcal{L}$  is a straight line of negative slope on a  $p, v$ -diagram for any given pair of values  $p_1, v_1$ . In view of conditions (5.9) for  $c_x$  it is clear that the Hugoniot relation  $\mathcal{H}_f$  defines another  $p, v$ -plane locus. Both  $\mathcal{L}$  and  $\mathcal{H}_f$  pass through the fixed point (or ‘origin’)  $p_1, v_1$  and any additional intersections of  $\mathcal{L}$  and  $\mathcal{H}_f$  define new pairs of  $(p, v)$ -values that describe changes across the frozen shock  $\mathcal{S}$ . Of course the actual jumps across  $\mathcal{S}$  will depend upon the character of the caloric equation of state (3.1). Despite this it is possible to make many general assertions about the changes that will occur across  $\mathcal{S}$  in gases. Hayes (1960) has discussed the matter in a very general way and a number of particular results that are relevant to the present topic, based on Hayes’ treatment, can be found in C & M.

One or two facts, that will be sufficient for present purposes, can be stated or illustrated as follows.

A typical  $\mathcal{H}_f$ -curve for a mixture of thermally perfect gases is depicted, together with some other Hugoniot-curves whose significance will be explained in due course, in figure 2. The tangent to  $\mathcal{H}_f$  at the origin is given by  $-\rho_1^2 a_{11}^2$  and the second derivative ( $\partial^2 p / \partial v^2$ ) on  $\mathcal{H}_f$  is positive. (This condition is only violated in gases for a number of high molecular weight hydrocarbons and fluorocarbons near to their

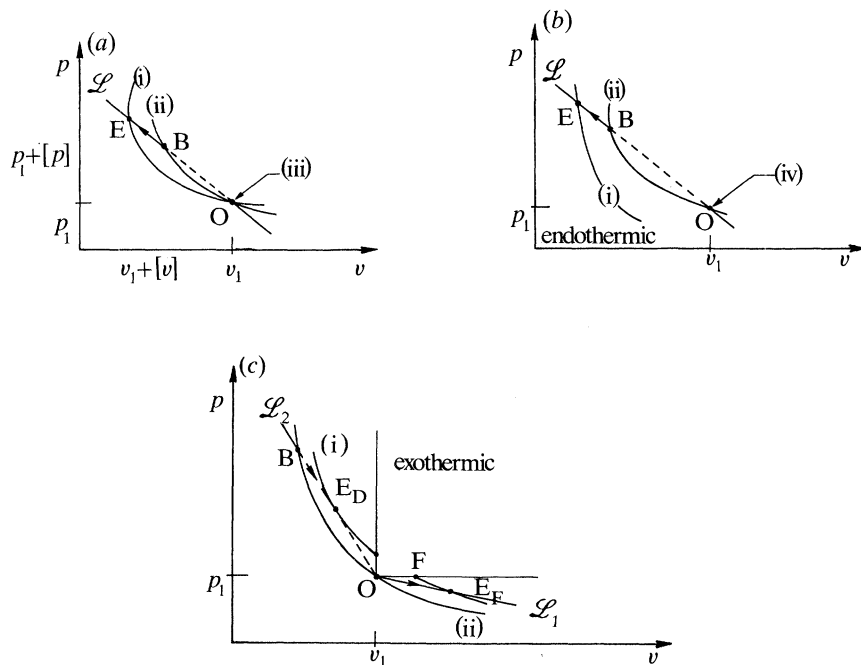


Figure 2. Hugoniot curves  $\mathcal{H}_e$ ,  $\mathcal{H}_r$  and Rayleigh lines  $\mathcal{L}$  on the  $(p, v)$ -diagram. (a) Shock OB propagating into an equilibrium atmosphere and initiating an endothermic reaction BE. (b) Shock OB propagating into a dis-equilibrium atmosphere and initiating an endothermic reaction. (c) Shock OB propagating into a dis-equilibrium atmosphere and initiating an exothermic (combustion) reaction  $BE_D$ ; a subsonic combustion wave (fast flame)  $OE_F$  propagating into the dis-equilibrium atmosphere. (i)  $\mathcal{H}_e$ , (ii)  $\mathcal{H}_r$ , (iii)  $c_1 = c_e(p_1, v_1)$ , (iv)  $c_{eq} \neq c_e(p_1, v_1)$ .

vapour-liquid phase boundary (Thompson & Lambrakis 1973.) Rayleigh line  $\mathcal{L}$  therefore only intersects  $\mathcal{H}_r$  twice, once at the 'origin' O and once again at B. Entropy at B is greater than (less than) entropy at O when  $[p] > 0$  ( $< 0$ ); hence compression shocks are permissible solutions of the Euler equations while expansion shocks are not. The differential increment of entropy on  $\mathcal{H}_r$  is given by

$$T ds = [v]^2 m dm, \quad (6.3)$$

so that  $s$  increases as the normal propagation speed (or mass flux) increases.

The minimum value of  $u_n$  is  $a_{r1}$ ; in other words the weakest frozen shock is an isentropic frozen sound wave. The shock strength  $[p]$  increases as normal propagation speed becomes supersonic relative to  $a_{r1}$ ; the normal component of the downstream speed must be subsonic relative to  $a_{r2}$ .

#### Extension of the definition of Hugoniot curves

The frozen shock produces instantaneous changes in  $p, v$  and hence, via (3.3), the temperature  $T$ . As a result  $\mathcal{S}$  will invariably act as a trigger to relaxational and chemical activity at faster rates than those that prevail ahead of the shock, since  $p$  and  $T$  increase across  $\mathcal{S}$  and chemical-reaction and other such rates increase with increasing molecular collision frequency and average collision energy.

In the implied circumstance of relatively rapid inputs to the flow field from source-terms downstream of  $\mathcal{S}$  one can proceed as follows. Consider first a special situation.

Assume that volume  $\mathcal{V}$  in §4 is of finite size and that surface  $\mathcal{A}$ , that surrounds it, consists in part of the surface of a parallel stream-tube, across which there is no flow, by hypothesis;  $\mathcal{A}$  is closed by a pair of stream-tube cross-sections that are perpendicular to the stream tube's axis. Conditions are uniform across any such cross-sections, the flow is one-dimensional, and jump conditions (5.5), (5.7) and (5.8) and the  $\mathcal{L}$ -relation (6.1) now apply to changes from the upstream section  $( )_1$  to the downstream section  $( )_2$  across a finite volume  $\mathcal{V}$  of fluid. Shock  $\mathcal{S}$  is assumed to lie just downstream of the  $( )_1$  section. The relation (6.2) is formally unchanged in present circumstances, but it is necessary to describe carefully what is meant by  $[h]$  since there is now time for any fluid element that crosses the volume  $\mathcal{V}$  to undergo significant changes as a result of inputs from the source terms.

For example, the flow may be driven to a new state of equilibrium by the time it reaches section  $( )_2$ . In such circumstances the jump in  $h$  (cf. (6.2)) must take account of the fact that all of the  $c_\alpha$  variables have local equilibrium values at section  $( )_2$ , and not the fixed  $( )_1$  values that are implicit in the designation  $\mathcal{H}_f$ . The new, equilibrium, value for

$$h_2 \equiv h(p_2, v_2, c_{\alpha e}(p_2, v_2)) \equiv h_{2\text{eq}}(p_2, v_2)$$

is acknowledged by the designation  $\mathcal{H}_e$  for the new Hugoniot. Figure 2 depicts some possible  $\mathcal{H}_e$  curves but shortens the notation for chemical state, etc., by just writing  $c = c_{\text{eq}}(p, v)$ , which is sufficiently suggestive at this stage.

Figure 2*a* depicts a particular case, for which the stream ahead of  $\mathcal{S}$  is itself in a state of equilibrium, since both  $\mathcal{H}_f$  and  $\mathcal{H}_e$  pass through the upstream state point at O. The plane steady phenomenon that is modelled by the sketch in figure 2*a* consists of a shock-jump from the equilibrium stream at O to conditions B, where composition is unchanged, followed by a 'relaxation-zone' from B to the new equilibrium state at E. The B to E transition is then a continuous change (of all of the flow, thermodynamical and chemical variables) that takes place along the Rayleigh line  $\mathcal{L}$ . As depicted in figure 2*a* it is an endothermic transition; in other words energy goes from the flow into the breaking of chemical bonds (dissociation) and/or into internal molecular energy modes. The physical distance that the flow must traverse between states B and E will, strictly, be arbitrarily large, with state E being approached exponentially slowly. However, for practical purposes, the transition distance or relaxation length can be roughly measured in units of  $a_f t_{\text{chem}}$  or, what is equivalent,  $\mathcal{R}l$  (cf. §2). Knudsen number  $Kn (=l$  divided by a body length  $L)$  is in the range  $10^{-1}$  to  $10^{-6}$  for a typical Shuttle re-entry, so that  $\mathcal{R}l$  can vary from a small fraction of  $L$  to many times that value.

The steady plane compression wave, whose structure has just been outlined briefly above, is about the most elementary finite-amplitude disturbance that can be found propagating into an equilibrium atmosphere of dissociating and relaxing gases. It is an odd fact that no wholly satisfactory analytical, or even acceptably-approximate analytical, solution for this quite basic element of a hypersonic flow field has been found (even for the simplest case of a single chemical reaction with no coupling to molecular vibration) until quite recently. A short account of this solution will be given in §10 below.

Figure 2*b* illustrates a generalization of the situation in figure 2*a*, specifically that the stream entering  $\mathcal{S}$  is assumed not to be in a state of equilibrium. The sketch suggests that  $\mathcal{H}_e$  will pass to the left of O and is, in this particular sense therefore, indicative of an endothermic reaction (cf. Hayes 1960). The relaxation region is still

B-to-E along  $\mathcal{L}$  and is formally the same as the continuous transition in figure 2a; only the initial conditions (at B) will be different.

Finally, figure 2c illustrates the situation when the final equilibrium Hugoniot  $\mathcal{H}_e$  is exothermic in character. Anything like a full discussion of the character of Hugoniot curves is out of the question in the present article. In the context of figure 2c, in particular, it is both simplest and sufficient, for present purposes, to assume that  $h$  is given by the elementary relation,

$$h = \mathcal{K}pv + cQ, \quad (6.4)$$

where  $\mathcal{K}$  is a pure number,  $Q$  is an energy of reaction per unit mass of the gas mixture and  $c$  is the fraction of the single reactant species in the flow that remains unburnt. Assuming that the reaction is simply a one-step chemically irreversible decomposition it follows that  $c_1 = 1$  and  $c_{\text{eq}} = 0$ . Therefore  $\mathcal{H}_e$  is actually a constant- $c$  locus, and some of the features of  $\mathcal{H}_f$  described above apply equally well to  $\mathcal{H}_e(c_{\text{eq}} = 0)$ .

One important condition for  $\mathcal{H}_e$  in figure 2c, that is additional to the ones already listed for  $\mathcal{H}_f$ , concerns points of tangency between  $\mathcal{H}$ -curves and  $\mathcal{L}$ -lines, usually called Chapman–Jouguet or CJ points. The downstream component  $u_{n2}$  of the flow-speed at such a point must be sonic, equal to  $a_{r2}$  in present circumstances (i.e. where  $c_{\text{eq}} = 0$ ).

Wave  $\text{OBE}_D$  in figure 2c consists of an  $\mathcal{S}$  shock-jump, O-to-B, followed by a continuous exothermic reaction-domain B-to- $\text{E}_D$ ; the latter is drawn as a CJ point in the figure. Since  $\mathcal{L}_2$  evidently represents a wave travelling at supersonic speeds relative to  $a_{r1}$  into gas ahead of  $\mathcal{S}$ , the whole wave represents the classical Zeldovich–von-Neumann–Döring (ZND) model of a planar CJ detonation.

Some combustion specialists assert that plane ZND waves are theoretical abstractions that ‘never’ occur in practice, even in laboratory shocktube experimental arrangements that are certainly more ‘one dimensional’ than most flows. One must have some sympathy with such assertions, but not so much as to decline to pay attention to the roles that plane or nearly-plane shocks and combustion waves (such as B-to- $\text{E}_D$  in figure 2c) can play in models of transient behaviour prior to establishment of (nominally) steady detonations. Extrapolation of some recent studies of essentially unsteady events to the present situation of steady (mostly) supersonic flows will be outlined in §11 below.

The Rayleigh line  $\mathcal{L}_1$  in figure 2c represents a plane wave that is travelling into unburnt material at subsonic speed ( $u_{n1} < a_{r1}$ ). The final point  $\text{E}_F$  represents a situation at the downstream end of the reaction wave, with completely burnt material emerging, still travelling at subsonic speed relative to the wave itself, at rather reduced pressure. It is important to note that the B-to- $\text{E}_D$  transition in figure 2c can be interpreted in precisely this same way, with B now acting in place of O as ‘origin’. It is becoming common to refer to reaction waves such as  $\text{OE}_F$  or  $\text{BE}_D$  as fast flames (Clarke 1989a). Whilst agreement on terminology is even more difficult to reach than agreement on scientific relevance amongst combustion scientists the designation fast flame for a subsonic-to-subsonic exothermic reaction wave such as  $\text{OE}_F$  will be used from now on in this article.

In passing it is worth remarking that the constant-pressure transition O-to-F on figure 2c is an acceptable approximation to the change in specific volume, and hence normal flow speed, across a Bunsen-burner type of premixed flame (Williams 1985). However, the change from O to F does not take place along  $\mathcal{L}_1$  for these very low-



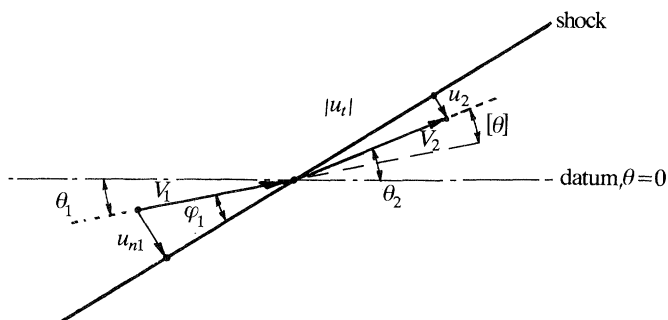


Figure 3. Notation for an oblique shock.

speed waves (typically  $u_{n1} \approx 10^{-3}a_{11}$ ), since their structure is controlled by diffusion and heat-conduction effects and these are explicitly excluded from the present article. Fast flames are essentially uninfluenced by any diffusive effects.

### Curved waves

The limitation to a purely plane, one-dimensional, geometry in the previous section on the extension of the definition of Hugoniot curves is severe but it is clear, on physical grounds at least, that the exact solutions from this special case are applicable, locally, as an approximation to two and three-dimensional flows provided that the radii of curvature of  $\mathcal{S}$ -wave and the streamlines downstream of  $\mathcal{S}$  are very large multiples of the reaction-zone thickness; the latter is roughly  $\mathcal{R}l$  (cf. §2). The dependence of  $l$  on pressure ( $pl \approx \text{const.}$ ) means that the idea of a shock-wave as a locally isolated and complete transition from one equilibrium condition to another (cf. figure 2a) is more likely to be encountered low down in the atmosphere, where pressures are highest, for given flow temperatures.

In general, of course,  $\mathcal{S}$ -waves are curved and the reaction zones behind them are then relatively complex in their interaction with the downstream flow. Curved  $\mathcal{S}$ -waves mean changes in mass flux  $m$  from place to place along the discontinuity surface, and (6.3) shows that variations of entropy  $s$  behind the shock will result. The consequences will be discussed in §9 below, after some more general results have been established for the behaviour of reacting flows.

## 7. Oblique shocks

Referring to figure 3 it can be seen that if  $\varphi_1$  is the angle between the stream ahead of a discontinuity  $\mathcal{S}$  and  $[\theta]$  is the jump in the flow angle measured from some suitable datum line in the plane of  $u_2$  and  $u_1$  then

$$\frac{\tan(\varphi_1 - [\theta])}{\tan \varphi_1} = \frac{u_{n2}}{u_{n1}} = \frac{v_2}{v_1} \equiv 1 + \frac{[v]}{v_1}. \quad (7.1)$$

The second relation follows from the continuity requirement (5.6) and it should be noted that all angles are acute, measured positive in the anti-clockwise direction from stream to shock  $\mathcal{S}$ . Since

$$m = \rho_1 u_{n1} = \rho_1 V_1 \sin \varphi_1 = \rho_2 V_2 \sin \varphi_2, \quad (7.2)$$

$$(6.1) \text{ shows that } [v]/v_1 = -[p]/\rho_1 V_1^2 \sin^2 \varphi_1, \quad (7.3)$$

whence (7.1) and (7.3) can be used to show that

$$\tan [\theta] = \cot \varphi_1 [p] (\rho_1 V_1^2 - [p])^{-1}. \quad (7.4)$$

Recalling that intrinsic energy  $e$  is formally, and quite generally, a function of  $p$ ,  $v$  and the sets of  $c_\alpha$  values, the  $\mathcal{H}$ -relation from (6.3) can be used, together with (7.3), to write

$$\left. \begin{aligned} &2e(p_1 + [p], v_1 - [p] (\rho_1 V_1 \sin \varphi_1)^{-2}, c_{\alpha 2}) \\ &- 2e(p_1, v_1, c_{\alpha 1}) - (2p_1 + [p]) [p] (\rho_1 V_1 \sin \varphi_1)^{-2} = 0. \end{aligned} \right\} \quad (7.5)$$

After some decision is made about the way in which  $c_{\alpha 2}$  relates to the upstream values  $c_{\alpha 1}$ , it can be seen that (7.5) is a relation that will give values for  $[p]$  for given upstream ( )<sub>1</sub> conditions including the  $\mathcal{S}$ -wave angle  $\varphi_1$ . The associated flow-deflection angle  $[\theta]$  will follow from (7.4).

If  $e$  does not depend upon  $c_\alpha$  and is, furthermore, simply proportional to the product  $pv$ , (7.5) reduces to the familiar direct expression for  $[p]$ , namely,

$$[p]/p_1 = (2\gamma/(\gamma + 1)) [M_1^2 \sin^2 \varphi_1 - 1], \quad (7.6)$$

where

$$M_1^2 \equiv V_1^2/a_1^2; \quad a_1^2 = \gamma p_1 v_1$$

and  $\gamma (= \mathcal{H}/(\mathcal{H} - 1))$ ; cf. (6.4) is the (implied) constant ratio of specific heats; in such circumstances  $a_1$  is the unique speed of sound ahead of  $\mathcal{S}$ .

When the gas is real, in the special sense that explicit account must be taken of the changes in  $c_\alpha$  across  $\mathcal{S}$ , the situation is evidently much less simple. It is clear that an important parameter in any relation between  $\varphi_1$  and  $[p]/p_1$  will be

$$\rho_1 V_1^2 \sin^2 \varphi_1 / p_1,$$

but  $[c_\alpha]$  will also play a role, as may the actual ( )<sub>1</sub> conditions themselves.

Returning to (7.6) for a moment, it is clear that  $[p] > 0$  only if  $M_1 \sin \varphi_1 > 1$ ; in other words  $\mathcal{S}$  will be a compression shock only if its speed of normal propagation into the gas ahead of the wave is supersonic. The arguments in favour of  $[p] > 0$  as the only acceptable  $\mathcal{S}$ -solution for inert flows, and forbidding solutions  $[p] < 0$ , are well known and can be put in two ways: (i) thermodynamic, based on the Second Law, exemplified by Hayes (1960), who made use of the thermodynamical character of the relevant  $\mathcal{H}$ -curve; (ii) mechanical, exemplified by the discussions of wave-structure that can be found in the book by Whitham (1974).

## 8. Continuous solutions

When the basic variables  $p$ ,  $\rho$ ,  $e$ ,  $u$ , and  $c_\alpha$  are continuous Gauss' theorem applied to (4.1)–(4.5) leads to the set of differential equations

$$\nabla \cdot (\rho \mathbf{u}) = 0, \quad (8.1)$$

$$\nabla \cdot (\rho \mathbf{u} \mathbf{u}) + \nabla p = 0, \quad (8.2)$$

$$\nabla \cdot (\rho \mathbf{u} h_0) = 0, \quad h_0 = h + \frac{1}{2} \mathbf{u} \cdot \mathbf{u}, \quad (8.3), (8.4)$$

$$\nabla \cdot (\rho c_\alpha \mathbf{u}) = K_\alpha, \quad \alpha = 1, 2, \dots, N. \quad (8.5)$$

These equations are in so-called divergence or conservation form, which can be helpful if it is intended to solve them by numerical finite-difference methods. The

source terms in (8.5) must, of course, be continuous functions of the physical variables; their presence signifies the most immediately apparent difference between the flow of either inert or fully-equilibrated mixtures and chemically-active gases.

As explained in §3 each and every  $K_\alpha$  can be expressed as a quotient, in which the numerator is expressive of a difference between actual local conditions and some chosen local equilibrium conditions whilst the denominator, having the dimensions of time, indicates the rapidity with which such departures from equilibrium may be reduced to zero (cf.  $t_{\text{chem}}$  in §2) if the local system is isolated from outside influences.

If the  $K_\alpha$  tend to vanish because their respective, ( $t_{\text{chem}}$ )-like, timescales are arbitrarily large relative to local flow times (in other words, if the relevant Damköhler number  $\mathcal{D} \rightarrow 0$ , cf. (2.6)) then the species equations (8.5) with the aid of (8.1), reduce to the statements

$$\mathbf{u} \cdot \nabla c_\alpha = 0. \quad (8.6)$$

Thus the  $c_\alpha$  will not change along streamlines and, in this particular sense, the flow will be inert or frozen. If the  $t_{\text{chem}}$  values or, more properly, the reciprocal of local Damköhler numbers, approach zero the numerators must do likewise in order to preserve the finite character of  $K_\alpha$ . Chemical and/or relaxational responses are then fast enough for the flow to proceed through a continuous sequence of states of local equilibrium. The differential equations (8.5) are replaced by algebraic relations that are derived by equating the numerator in  $K_\alpha$  to zero; rates of change of  $c_\alpha = c_{\alpha\text{eq}}$  along streamlines can eventually be found from the values of  $\mathbf{u} \cdot \nabla c_{\alpha\text{eq}}$  if they should be required.

The task of solving the complete set of equations (8.1)–(8.5) is greatly reduced for both inert and equilibrium flows by virtue of the consequent simplifications in (8.5). However, even these solutions are not wholly straightforward, especially for equilibrium flows where the relatively complicated ways in which the  $c_{\alpha\text{eq}}$  depend upon  $p$  and  $v$ , for example, invariably make  $h_{\text{eq}}(p, v)$  an awkward function; this usually presents insuperable obstacles to progress by purely analytical means and can also pose some problems for modern computational numerical methods.

#### *Natural coordinates and characteristics*

The vector notation in (8.1)–(8.5) has the merit of brevity but it is often more instructive to write out the various operations in those equations in full for some chosen coordinate system. One such especially instructive system for planar two-dimensional flows is the orthogonal curvilinear net made up of streamlines and normals that is sometimes called the natural system of coordinates. A similar remark applies to axially symmetric flows but they are left as an exercise for the reader (or see Emanuel 1986, ch. 13).

Write the differential increments of displacement along streamlines and normals as  $\sigma_1 d\xi_1$  and  $\sigma_2 d\xi_2$ , respectively, so that the  $\sigma_n$  ( $n = 1, 2$ ) are scale factors. Then (8.1), (8.2) and (8.3) become, respectively,

$$\rho V \sigma_2 = \bar{m}(\xi_2), \quad (8.7)$$

$$\rho V V_{\xi_1} + p_{\xi_1} = 0, \quad (8.8)$$

$$\rho V^2 (1/\sigma_1) \theta_{\xi_1} + (1/\sigma_2) p_{\xi_2} = 0, \quad (8.9)$$

$$h + \frac{1}{2} V^2 = H(\xi_2). \quad (8.10)$$

The functions  $\bar{m}(\xi_2)$  and  $H(\xi_2)$  are functions of integration of (8.1) and (8.3), which

reduce to statements that  $\rho V \sigma_2$  and  $h_0$  do not vary with  $\xi_1$ ;  $V$  is the magnitude of the velocity vector (identical with  $|\mathbf{u}|$ , of course) and  $\theta$  is the flow-deflection angle measured from some datum-direction, often the free-stream.

The species equations (8.5) become

$$\rho V c_{\alpha \xi_1} = \sigma_1 K_\alpha. \quad (8.11)$$

Conservation relations, (8.7)–(8.11), must be augmented by some purely geometric information about the way in which the scale factors  $\sigma_n$  depend upon local flow geometry, namely

$$\sigma_{2 \xi_1} = \sigma_1 \vartheta_{\xi_2}, \quad (8.12)$$

$$\sigma_{1 \xi_2} = -\sigma_2 \vartheta_{\xi_1}. \quad (8.13)$$

Any attempt to solve the equations in a streamline-and-normal system must recognize, implicitly or explicitly, that  $\sigma_1$  and  $\sigma_2$  are two more dependent variables. This situation is often implicit (cf. Liepmann & Roshko 1957, §7.9) in the sense that  $\sigma_1 d\xi_1$  and  $\sigma_2 d\xi_2$  are written as differential increments of length, such as  $dS$  and  $dN$  for example; in this article the fact is exhibited explicitly, for purposes that will appear in a section to follow that outlines a numerical computational method.

If (8.7) and (8.10) are differentiated with respect to  $\xi_1$  the results can be combined with (8.8) to show that

$$(M_f^2 - 1) \frac{1}{\sigma_1} p_{\xi_1} + \rho V^2 \frac{1}{\sigma_2} \vartheta_{\xi_2} = \mathbb{K} \frac{1}{\sigma_1}, \quad (8.14)$$

where

$$\mathbb{K} \equiv - \left\{ \frac{V \sigma_1}{\rho a_f^2 e_p} \right\} \sum_{\alpha=1}^{N-1} \left( \frac{\partial h}{\partial c_\alpha} \right)_{p, \rho, c_\beta} K_\alpha,$$

$$e_p \equiv \left( \frac{\partial e}{\partial p} \right)_{\rho, c_\alpha},$$

$$M_f \equiv V/a_f.$$

The local frozen sound speed  $a_f$  is defined in §3, and  $M_f$  is evidently the local Mach number based on this particular limiting value of the continuum of possible signal speeds.

Defining the frozen Mach angle  $\mu_f$  via

$$M_f \sin \mu_f = 1 \quad (8.15)$$

combination of (8.9) and (8.14) leads to the results

$$\cot \mu_f (dp/d\xi_1) \pm \rho V^2 (d\vartheta/d\xi_1) = \mathbb{K} \tan \mu_f, \quad (8.16)$$

where the operators

$$\frac{d}{d\xi_1} \equiv \frac{\partial}{\partial \xi_1} \pm \tan \mu_f \left( \frac{\sigma_1}{\sigma_2} \right) \frac{\partial}{\partial \xi_2} \quad (8.17)$$

define two families of characteristic lines,  $\chi_l = \text{const.}$  or  $\chi_r = \text{const.}$ , such that

$$\frac{\sigma_2}{\sigma_1} \left( \frac{\partial \xi_2}{\partial \xi_1} \right)_{\chi_{l,r}} = \pm \tan \mu_f. \quad (8.18)$$

It is clear from (8.8) or (8.10) and particularly from (8.11), for example, that streamlines are also characteristics of the system. Provided that the flow is

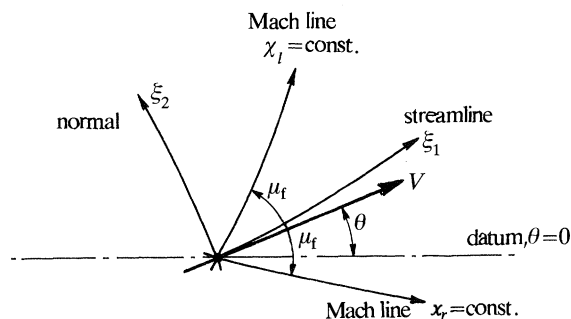


Figure 4. Streamline and normal (orthogonal curvilinear) coordinate system and characteristics.

supersonic, in the strict sense that  $M_f \geq 1$  (cf. (8.15)), it can be seen that the network of frozen Mach lines is also characteristic. In such circumstances the flow equations are totally hyperbolic. Figure 4 illustrates the disposition of the various characteristic and coordinate lines.

#### *Similitudes and natural coordinates*

One of the great facilitators of calculation in planar supersonic or hypersonic flows of inert gases is the existence of similarity solutions of equations like those in the previous subsection. These simple-wave flows (cf. Courant & Friedrichs 1948) are usually derived in the context of cartesian geometries but, for present and subsequent purposes, it is interesting to enquire briefly how investigation of such similitudes might proceed in the natural orthogonal curvilinear coordinates of this section.

The question is therefore posed; 'Are there solutions for all of  $p, \rho, \theta, V, \sigma_1$  and  $\sigma_2$  that can be expressed as functions of the single variable  $\eta$ ?', where

$$\eta \equiv \xi_2/\xi_1. \quad (8.19)$$

The origin for  $\xi_{1,2}$  can be chosen anywhere within the field of flow, so the arguments that follow are quite general.

For any variable  $f = f(\eta)$  it follows that

$$\frac{df}{d\xi_1} = \left\{ -\eta \pm \frac{\sigma_1}{\sigma_2} \tan \mu_f \right\} \frac{df}{d\eta} \frac{1}{\xi_1}. \quad (8.20)$$

The factor  $\xi_1$  can only be cancelled from (8.16) if  $\mathbb{K} \tan \mu_f$  is equal to a function of  $\eta$  divided by  $\xi_1$ , which in general it plainly is not, or if  $\mathbb{K}$  vanishes identically. The latter implies that each and every  $K_\alpha$  must vanish; in other words the flow must be chemically inert. (For brevity the equilibrium situation  $c_\alpha \equiv c_{\alpha eq}$ , which also admits similitudes, is omitted here. It is instructive to see how matters turn out when  $\sigma_1 K_\alpha = \rho V \partial c_{\alpha eq} / \partial \xi_1$  in  $\mathbb{K}$ , but the details are left for the reader to pursue for him or herself.)

It must be concluded that similitude solutions, or simple waves, do not exist in flows with finite-rate reactions in them. This result actually extends to situations within which source terms of any kind are operative.

It is worth noting, however, that if  $\mathbb{K}$  does vanish then all of  $p, \rho, \theta, V, \sigma_1$  and  $\sigma_2$  can be constant on lines of constant  $\xi_1/\xi_2$  for plane steady supersonic or hypersonic

flows. The similitude forms of the two equations (8.16) can now be seen, with the aid of (8.20), to be satisfied in a non-trivial way (i.e.  $p$  and  $\theta$  not constant everywhere in some finite neighbourhood) by making

$$\eta = \pm (\sigma_1/\sigma_2) \tan \mu_r \quad (8.21)$$

and

$$\cot \mu_r dp/d\eta \mp \rho V^2 d\theta/d\eta = 0, \quad (8.22)$$

where, as usual, it is necessary to take either upper or lower signs together in the equations.

Comparison of (8.18) with (8.21) shows that in the circumstances lines  $\eta = \text{const.}$  are characteristics (frozen Mach lines) and, furthermore, that they are straight lines in the  $\xi_1, \xi_2$ -plane. It will shortly be seen how these various facts can be turned to advantage in the treatment of some reacting flows.

In simple ideal gases the quantity  $(\cot \mu_r/\rho V^2) dp$  is integrable; it is called the Prandtl–Meyer function and is usually quoted in terms of local Mach number and a (constant) ratio of specific heats (Liepmann & Roshko 1957, §4.10). The more complex thermodynamical relationships that are necessary to account for flow behaviour at very high temperature levels are usually such as to make it impossible to achieve this kind of an analytical result.

Whatever may be the case, a particular solution from (8.21) and (8.22) can consist of a ‘fan’ of characteristics  $\eta = \text{const.}$  that spring from a single point. Such a solution must represent a wave of expansion, or rarefaction for any fluid element that travels through the wave along a streamline  $\xi_2 = \text{const.}$  These will be called  $\mathcal{R}$ -waves from now on.

#### *A numerical computational method*

It is evident that the presence of source terms in the conservation equations leads to difficulties with their solution. Analytical solutions are out of the question and approximate analytical theories are of rather limited practical, as opposed to pedagogical, value. A fairly full account of small-disturbance theories was given by the writer some years ago (Clarke 1969) and one or two more recent, and quite different, efforts in the field of analytical-approximate theories have recently been made by Mughal (1989).

A numerical method, that is somewhat outside the mainstream of current computational studies, that makes use of some of the results that have been presented here so far, and is capable of producing some useful results for finite-rate chemistry in planar steady two-dimensional supersonic ( $M_f \geq 1$ ) flows, is based, first and foremost, on the idea of ‘operator splitting’ (see, for example, Strang 1968).

Representing the conservation equations symbolically as

$$NU = S,$$

where  $U$  is a vector of conserved quantities,  $N$  is a nonlinear differential operator and  $S$  is the vector of algebraic source terms, a finite-difference solution is constructed in steps, as follows. First solve what can be called the wave problem  $NU_w = 0$  in a small element of  $\xi_1, \xi_2$  space to find a solution  $U_w$  with  $c_\alpha = \text{const.}$  along streamlines and then use  $U_w$  to help set up and subsequently solve a simpler source problem  $N_s U = S$  with which to up-date and correct  $U_w$  for the effects of chemical action. In the natural coordinate system operator  $N_s$  is clearly best limited to differentiations in the streamline direction  $\xi_1$ , thus taking full advantage of the simple character of (8.11). Solutions march downstream in the  $\xi_1$  direction and, of course, it is necessary to include  $\sigma_1, \sigma_2$  in the collection of dependent variables.

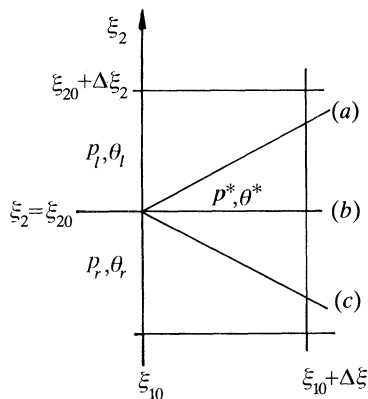


Figure 5. A Riemann problem in  $\xi_1 \xi_2$  space. Data on  $\xi_1 = \xi_{10}$  is piecewise constant and gives rise to a solution that consists of waves  $\mathcal{W}_m$  ( $m = l$  (a) or  $r$  (c)) that may be shocks  $\mathcal{S}$  or rarefactions  $\mathcal{R}$ ; (b)  $\mathcal{W}_c$  is always a contact discontinuity  $\mathcal{C}$ .

Solution of the wave-problem can exploit the information about slip surfaces  $\mathcal{C}$  (§5), plane oblique shocks  $\mathcal{S}$  (§7) and similitude solutions in  $\xi_1, \xi_2$ -space (see above) to deal with discretized data, along a  $\xi_2$ -normal in the flow, as a sequence of Riemann-type problems in the natural coordinate space. Briefly the procedure is as follows. Consider a small region in  $\xi_1, \xi_2$  space; assume that pressure  $p_l$  and flow angle  $\theta_l$ , etc., are uniformly constant in  $\xi_2 > \xi_{20}$  (see figure 5) and, in general, different from similarly constant values in  $\xi_2 < \xi_{20}$ . The solution of this initial-value problem will consist of three centred waves,  $\mathcal{W}_l, \mathcal{W}_c$  and  $\mathcal{W}_r$  as depicted in figure 5. Any wave  $\mathcal{W}_{l,r}$  that is not  $\mathcal{S}$  behaves like the  $\mathcal{R}$ -waves described above;  $\mathcal{W}_c$  will always be a slip-surface  $\mathcal{C}$  and will always lie along  $\xi_2 = \xi_{20}$ .

The Riemann problem is to find  $\mathcal{W}_{l,r}$  such that  $[p] = 0 = [\theta]$  at  $\mathcal{W}_c$ .

If  $\theta$  jumps or changes by an amount  $[\theta]_{l,r}$  across  $\mathcal{W}_{l,r}$ , respectively, the condition  $[\theta] = 0$  across  $\mathcal{W}_c: \mathcal{C}$  is just

$$\theta_l + [\theta]_l = \theta_r + [\theta]_r$$

or

$$[\theta]_l - [\theta]_r = (\theta_r - \theta_l) \equiv \Delta\theta. \quad (8.23)$$

Condition  $[p] = 0$  at  $\mathcal{W}_c: \mathcal{C}$  is met by making the pressure downstream of  $\mathcal{W}_l$  and  $\mathcal{W}_r$  equal to  $p^*$ , as implied in figure 5.

If a relation between  $[\theta]_{l,r}$  and  $[p]_{l,r}$  can be found that involves only given conditions on  $\xi_1 = \xi_{10}$  it is clear that (8.23) provides a relation from which  $p^*$  can be calculated. When this is done the Riemann problem is solved.

Referring to §7, note first that the subscript-1 states will be either  $l$  or  $r$  states in figure 5. First select  $c_{\alpha 2} = c_{\alpha 1}$  in (7.5) (note that  $c_\alpha$  will normally not be the same in  $l$  and  $r$  states); choice of  $[p]$  in (7.5) will give  $\sin \beta_1$  whence, with  $\beta_1$  necessarily an acute angle, (7.4) will give the associated  $[\theta]$ , and the requisite  $[\theta]_{l,r}$  against  $[p]_{l,r}$  relations therefore exist for  $\mathcal{S}$ -waves.

The centred expansion waves described by (8.22) are isentropic when  $c_\alpha$  is fixed, so that these equations give the  $\mathcal{R}$ -wave  $[p], [\theta]$  relation via

$$\int_{p_m}^{p_m + [p]_m} (\cot \mu_1 / \rho V^2) \partial_s p \pm [\theta]_m = 0, \quad m = l, r, \quad (8.24)$$

where  $\partial_s p$  signifies integration with respect to pressure  $p$  at fixed entropy  $s$ . The fact

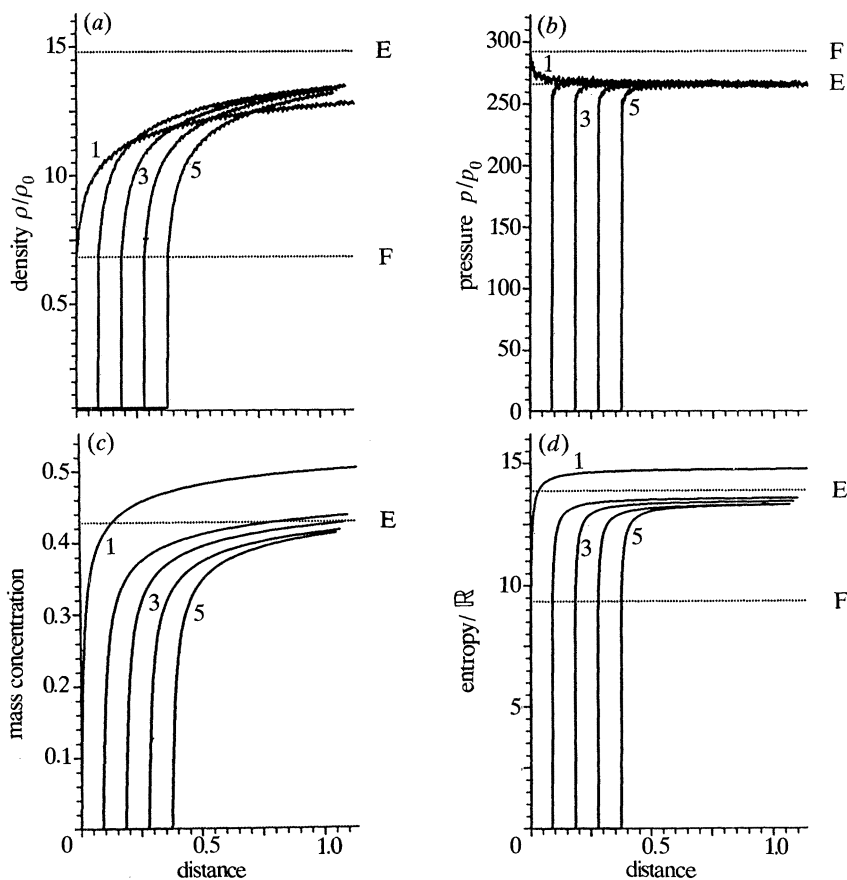


Figure 6. Some results for the flow of an ideal dissociating gas (Lighthill 1957) past a wedge with an attached shock calculated by the methods outlined in §8. The frozen Mach number of the undissociated free-stream is 32 and the shock-wave angle  $\varphi_1$  (cf. figure 3) at the apex of the wedge is  $30^\circ$ . Curves 1–5 in the figures show variations of (a) density, (b) pressure, (c) mass fraction and (d) entropy with ‘distance’ measured along each one of five streamlines; curves 1 apply to a streamline just above the surface of the wedge, while 2, 3, 4 and 5 show variations along streamlines above the surface that are situated so as to enclose similar increments of mass-flux between adjacent pairs. Dotted lines E, F denote wholly-equilibrium and wholly-frozen flow conditions. The existence of a layer adjacent to the surface across which entropy, composition and density all vary significantly, is evident.

that one needs to know  $e$  as a function of  $p, v$  and the  $c_\alpha$  in order to solve the  $\mathcal{S}$ -wave problem, and  $e$  or  $h$  as a function of  $p, s$  and the  $c_\alpha$  does not make matters any easier, even in the context of the present, simpler, ‘split’ problem. However there is no serious obstacle in the way of progress via numerical computation and figure 6 depicts some results that have been obtained by A. S. Dawes (personal communication) using the techniques whose broad character has been outlined above.

Computation in a natural coordinate system had advantages in the specification of boundary-conditions (e.g.  $\theta = \theta_b(\xi_1)$  on  $\xi_2 = 0$ ), and the obvious location of slip surfaces  $\mathcal{S}$ . The clear-cut character of operator-splitting for reacting flows is also attractive and, apart from the work by Dawes, has not been exploited to date.

There is quite a range of choice for the way in which solutions of individual Riemann problems can be used to provide data at the ‘new’  $\xi_1$ -value; for example,



random choice (the method used by Dawes), weighted-average flux (Toro 1989), etc., but this is not the place to go into such detail and, in any case, developments are taking place at such great speed in the whole field of computational studies that any value-judgement is likely to be superceded by another before it appears in print.

The disadvantage of the numerical method that has just been described is, plainly, its restriction to supersonic ( $M_t > 1$ ) flows. As a result blunt bodies cannot be treated by this technique, but it is possible to acquire some useful information about the influence of finite-rate chemistry on such things as trailing-edge controls and engine-inlets, which are situated at the downstream end of quite long runs of predominantly supersonic reacting flow, and rather distant from the patches of subsonic flow that exist in the neighbourhood of stagnation points or lines at leading edges.

## 9. Vorticity

A further feature of hypersonic flows with finite-rate chemical change, that is implicit in various parts of the text so far, but which must now be made explicit, is their association with vorticity. Euler models of any steady flow behaviour must obey the momentum equations

$$\mathbf{u} \cdot \nabla \mathbf{u} = \frac{1}{2} \nabla (\mathbf{u} \cdot \mathbf{u}) - \mathbf{u} \times \boldsymbol{\omega} = -v \nabla p, \quad (9.1)$$

where  $\boldsymbol{\omega} \equiv \nabla \times \mathbf{u}$  is the vorticity. Taking the vector curl of the second version of this relation shows that

$$\mathbf{u} \cdot \nabla \boldsymbol{\omega} - \boldsymbol{\omega} \cdot \nabla \mathbf{u} + \boldsymbol{\omega} (\nabla \cdot \mathbf{u}) = -\nabla v \times \nabla p. \quad (9.2)$$

Since mass-conservation requires  $\nabla \cdot (\rho \mathbf{u})$  to vanish, (9.2) leads directly to the result (NB  $v = 1/\rho$ )

$$D(v\boldsymbol{\omega})/Dt = v\boldsymbol{\omega} \cdot \nabla \mathbf{u} - v \nabla v \times \nabla p, \quad (9.3)$$

where  $D(v\boldsymbol{\omega})/Dt$  is the rate of change of  $v\boldsymbol{\omega}$  following the motion of a material point, namely  $\mathbf{u} \cdot \nabla (v\boldsymbol{\omega})$  in a steady flow.

The first term on the right-hand side of (9.3) describes the local instantaneous spatial rate of change of the flow-velocity vector in the direction of the vortex line, so that  $v\boldsymbol{\omega}$  for a fluid particle changes as a result of the action of such instantaneous local strain rates. The twisting and stretching of a vortex line that is described by the term  $v\boldsymbol{\omega} \cdot \nabla \mathbf{u}$  is only active in three-dimensional flows since the term vanishes in plane flow.

The fact that an infinitesimal line-element  $d\mathbf{l}$  that is made up of material points obeys the relation  $D(d\mathbf{l})/Dt = d\mathbf{l} \cdot \nabla \mathbf{u}$  can be used to prove that vortex lines follow material points, and therefore move with the fluid, but only when  $\nabla v \times \nabla p$  vanishes from (9.3) (Batchelor 1967, pp. 131–132; Whitham 1963, pp. 121–124). In addition to the case of incompressible flow, for which  $\nabla v = 0$ ,  $\nabla v \times \nabla p$  will also vanish when the two gradient vectors are colinear, which is what happens when  $p$  is a function of  $v$  only. There are many situations in the flow of compressible fluids for which  $p = p(v)$  is either true or sufficiently nearly so to make  $\nabla v \times \nabla p = 0$  an acceptable approximation. However, these situations demand that the flow shall be both homentropic ( $\nabla s = 0$ ) and of fixed chemical composition ( $\nabla c_\alpha = 0 \forall \alpha$ ) and, on the whole, neither of these conditions is satisfied in a hypersonic flow, as will now be demonstrated.

Expressing  $v$  as a function of pressure  $p$ , entropy  $s$ , and chemical composition  $c_\alpha$ , it is clear that

$$\nabla v = \left(\frac{\partial v}{\partial p}\right)_{s, c_\alpha} \nabla p + \left(\frac{\partial v}{\partial s}\right)_{p, c_\alpha} \nabla s + \sum_{\alpha=1}^N \left(\frac{\partial v}{\partial c_\alpha}\right)_{p, s, c_\beta} \nabla c_\alpha. \quad (9.4)$$

It follows from (3.9) and equations (8.1), (8.2) and (8.3), which can be combined to give

$$\mathbf{u} \cdot \nabla h - v \mathbf{u} \cdot \nabla p = 0,$$

that

$$\rho T \mathbf{u} \cdot \nabla s = - \sum_{\alpha=1}^N \mu_\alpha K_\alpha \quad (9.5)$$

where (8.4) has been used to eliminate  $\mathbf{u} \cdot \nabla c_\alpha$ . The right-hand side of (9.5) must be positive, unless the flow is either frozen or in a state of permanent equilibrium, when it will vanish. Such a thing is obvious from the Second Law of Thermodynamics and the fact that reactions are natural processes; a demonstration of the validity of the statement, that sheds some additional light on the relationships between  $\mu_\alpha$  and  $K_\alpha$  can be found in §1.14 of C & M.

Therefore, in those parts of the flow field for which the variables are continuous, (9.5) shows that entropy is continuously created by chemical activity within any fluid element as it moves along its streamline. As a consequence  $\nabla s$  is unlikely to vanish anywhere within the field; the same must be true for  $\nabla c_\alpha$ .

Thus  $\nabla v \times \nabla p$  does not vanish and (9.3) show that vorticity is continuously created or destroyed, depending on the sign of  $\nabla v \times \nabla p$ , in any given element of the gas mixture, whether the motion be two dimensional or three dimensional.

In any flow field for which shocks appear, which in essence means all hypersonic flows, it is crucial to recall that entropy increases across  $\mathcal{S}$ -waves by amounts that change with variations in the normal mass flux  $m$  (see (6.3)). As a result a very important contribution to  $\nabla s$  is associated with curved shock waves  $\mathcal{S}$ , that is to say, with one of the discontinuous features of solutions of the Euler equations. It can be demonstrated (as in §10 below) that chemical activity downstream of a shock wave will lead to curvature of that wave, regardless of any part that may be played by the geometric effects of body shape. The latter will be experienced in the flow around hypersonic vehicles when leading edges of the vehicle are made blunt to avoid excessive local heat transfer rates.

The question of shock shape and vorticity will be taken up again shortly, after another important relation between vorticity and flow-field features has been described.

**Crocco's Theorem.** *Rewriting (9.1) as*

$$\mathbf{u} \times \boldsymbol{\omega} = v \nabla p + \frac{1}{2} \nabla (\mathbf{u} \cdot \mathbf{u}),$$

(3.9) can be used to show that

$$\mathbf{u} \times \boldsymbol{\omega} = -T \nabla s + \nabla (h + \frac{1}{2} \mathbf{u} \cdot \mathbf{u}) - \sum_{\alpha=1}^N \mu_\alpha \nabla c_\alpha. \quad (9.6)$$

This last relation is a general form of what is usually referred to as Crocco's Theorem or Law. In the present context, the direct contributions arising from chemical change are noteworthy; their additional strong connections with  $\nabla s$  will be described a little more thoroughly in due course.

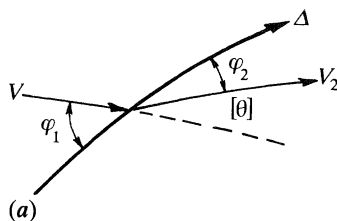


Figure 7. Distance  $\Delta$  measured along a curved shock wave and other notation.  
(a)  $\mathcal{S}$ : shock wave.

When the flow is steady it has already been remarked in §8 that stagnation enthalpy  $h + \frac{1}{2}\mathbf{u} \cdot \mathbf{u} \equiv h_0$  does not vary along a streamline. It is also usually the case, certainly for theoretical models of flight in the atmosphere, that  $h_0$  is presumed to have the same value on every streamline. As a result (9.6) simplifies to

$$\mathbf{u} \times \boldsymbol{\omega} = -T\nabla s - \sum_{\alpha=1}^N \mu_{\alpha} \nabla c_{\alpha}, \quad (9.7)$$

which reinforces the very direct nature of the connection between entropy and composition gradients and local vorticity values.

#### *Vorticity and curved frozen shocks*

It is simplest to consider the relation between vorticity and curved  $\mathcal{S}$ -shocks in the natural coordinate system introduced in §8. An immediate consequence of the restriction to plane flows is that (9.5) and (9.7) combine to give

$$\sigma_2 V \zeta = T \frac{\partial s}{\partial \xi_2} + \sum_{\alpha=1}^N \mu_{\alpha} \frac{\partial c_{\alpha}}{\partial \xi_2}, \quad (9.8)$$

where  $\zeta$  is the sole surviving component of  $\nabla \times \mathbf{u}$ . In other words, only gradients of entropy and composition that are normal to streamlines are significant for the existence of vorticity.

The result in (9.8) is only valid in the continuous parts of the flow, but these include the regions immediately upstream and downstream of a discontinuous  $\mathcal{S}$ -wave. It can be seen from figure 7 that combination of (3.7) and (9.8) gives

$$\sin \varphi_2 V_2 \zeta_2 = -\{\partial h_2 / \partial \Delta - v_2 \partial p_2 / \partial \Delta\},$$

for the flow immediately downstream of  $\mathcal{S}$ , where  $\varphi_2$  is the local acute angle between  $\mathcal{S}$  and the streamline, and  $\Delta$  is distance measured along  $\mathcal{S}$ . Since the shock is curved,  $\varphi_2$  will vary with  $\Delta$ .

Using the relations from (6.1) and (6.2) to write

$$h_2 = h_1 - \frac{1}{2}m^2(v_2^2 - v_1^2)$$

it can be shown, after some elementary manipulations, that

$$\sin \varphi_2 V_2 \zeta_2 = \sin \varphi_1 V_1 \zeta_1 - [v] \left\{ \frac{\partial p_1}{\partial \Delta} + m^2 \frac{\partial v_1}{\partial \Delta} \right\} + [v]^2 m \frac{\partial m}{\partial \Delta}. \quad (9.9)$$

This relation gives the vorticity  $\zeta_2$  downstream of a curved shock in terms of the vorticity  $\zeta_1$  and the state of the flow upstream of the shock, together with its shape

(specifically  $\varphi_1$  against  $\Delta$ , since  $\varphi_2$  is derivable from a knowledge of the subscript-1 conditions, as shown in §7).

Conditions ahead of a shock-wave are not necessarily either uniform or irrotational, but if they are (9.9) reduces to the statement that

$$\zeta_2 = \frac{[v]^2 m}{V_2 \sin \varphi_2} \frac{\partial m}{\partial \Delta} = V_1 \frac{(1-r)^2}{r} \cos \varphi_1 \frac{\partial \varphi_1}{\partial \Delta}. \quad (9.10)$$

The last result here follows from results that can be found in §7;  $r$  is written for the density ratio

$$r \equiv \rho_1/\rho_2 \equiv v_2/v_1; \quad (0 < r \leq 1). \quad (9.11)$$

The last version of (9.10) can be recognized as the frequently quoted result from Hayes & Probstein (1966, equation (1.5.12)), that makes the attractively direct connection between  $\zeta_2$  vorticity and shock curvature  $\partial \varphi_1/\partial \Delta$ .

The atmosphere into which a hypersonic vehicle travels is usually uniform and irrotational in character, so that (9.10) applies to the front or bow shock-waves in such a case. Furthermore  $r$  is often less than  $10^{-1}$  in magnitude; the factor  $(1-r)^2 r^{-1}$  is therefore large and  $\mathcal{S}$ -wave generation of vorticity is rather effective for bow shocks.

Re-writing (9.9) in light of (7.2) and definition (9.11) shows that

$$\zeta_2 = \frac{1}{r} \zeta_1 + \left(\frac{1}{r} - 1\right) \left\{ \frac{1}{m} \frac{\partial p_1}{\partial \Delta} + m \frac{\partial v_1}{\partial \Delta} \right\} + \left(\frac{1-r}{r}\right)^2 \left( \frac{1}{\rho_1} \frac{\partial m}{\partial \Delta} \right). \quad (9.12)$$

This result will apply in most practical hypersonic circumstances to curved shock-waves that appear in the disturbed flow field downstream of a strong bow wave. These shocks will therefore be weaker, and  $r$  consequently nearer to unity, than in the case of the bow wave. It is interesting to see, from the first term in (9.12), how simple compression will amplify vorticity (cf. (9.3)). Comparison of the last term in (9.12) with the result in (9.10) is also instructive.

## 10. Shocks and associated chemical activity

Nothing has yet been said in any detail about the way in which chemical activity develops from the point where it is initiated or, perhaps, strongly perturbed, by the appearance of an  $\mathcal{S}$ -wave, except for some assertions about the general nature of transitions B-to-E in the early parts of §6 (cf. figure 2 in particular). Even these few remarks are, strictly, limited to plane waves which, of course, constitute a very special case and may not generally be encountered in hypersonic flow fields. This section will attempt to describe in more detail how chemical changes proceed in, and interact with, flow downstream of  $\mathcal{S}$ -waves, starting with the simplest case of a normal shock.

### *Normal shock in a simple dissociating gas*

It has already been remarked in §6 that no acceptably accurate approximate solution exists, even for the simplest case of a single dissociation reaction that is initiated by a plane  $\mathcal{S}$ -wave in a pure homonuclear diatomic species. This state of affairs has been put right recently by Birkhan *et al.* (1988) and a brief account of their method will be given shortly. It should be remarked that the work of Birkhan *et al.* assumed that density is constant in a mixture consisting of heteronuclear molecules

AB, plus the separate A and B atoms. At the initial instant of time these authors assume that temperature is suitably high, with all A and B atoms absent; dissociation of AB proceeds immediately from the chosen initial conditions. The process is therefore one of temporal evolution in a system that is spatially uniform. The method is readily adaptable to present needs, which are for an account of spatial development in a steady state downstream of a plane  $\mathcal{S}$ -wave. Some simplification is afforded by treating dissociation and recombination in a homonuclear molecule  $A_2$ . Equation (8.11) can then be written in the form

$$c_{\xi_1} = (\sigma_1/\tau_d V)\{[1-c]-c^2(\rho/\rho_d)\exp(\vartheta_d/T)\}, \quad (10.1)$$

where  $c$  is atom mass fraction and where  $\vartheta_d$ ,  $\rho_d$  and  $\tau_d$  are thermodynamical and chemical kinetic parameters or variables for the specific mixture of  $A_2$  molecules and A atoms, defined as follows. Note that  $(\sigma_1/V\tau_d)$  is the local Damköhler number.

If  $D$  is the energy required to dissociate unit mass of molecules at the absolute zero of temperature, and  $W_2$  is the molecular weight of the molecules,

$$\vartheta_d \equiv DW_2/\mathbb{R}; \quad (10.2)$$

$\rho_d$  is a characteristic dissociation density, a weak function of temperature that is assumed to be constant in Lighthill's (1957) model of an ideal dissociating gas. Typical values of  $\vartheta_d$  and  $\rho_d$  are those for oxygen, namely  $5.9 \times 10^4$  K and  $1.5 \times 10^5$  kg m<sup>-3</sup>; the ratio of  $\rho_d$  to  $\rho$ , the density in a typical flow field, is large and lies between  $10^5$  and  $10^7$ , as a rough guide, for many applications. The group of terms  $(\rho/\rho_d)\exp(\vartheta_d/T)$  can therefore take values around unity for temperatures measured in units of  $10^3$  K and, as can be seen from (10.1), equilibrium values of  $c$  will do the same.

The chemical (specifically in this case dissociation) time  $\tau_d$  is given by

$$1/\tau_d = \Omega \exp(-\vartheta_d/T). \quad (10.3)$$

The pre-exponential factor  $\Omega$  has a magnitude that is about the same as the frequency of intermolecular collisions. The exponential factor in (10.3) acknowledges, in the manner of Arrhenius, that there is an activation energy for the dissociation reaction that is in this case equal to the dissociation energy itself. By comparison with the exponential,  $\Omega$  is a weak function of temperature but it does also depend upon density or pressure, being proportional to  $p$  for example.

Clearly (10.1) involves  $V$ ,  $T$  and  $\rho$  as well as  $c$ ; it can be seen from equations such as (8.7), (8.8) and (8.10), specialized to apply to the present plane-flow situation (namely  $\sigma_2$ ,  $\bar{m}$  and  $H$  equal to constants) that relatively simple linear relations exist between all of these quantities but, even so, (10.1) is still impossible to solve analytically in view of its strong nonlinearity.

It will be assumed that the atmosphere ahead of  $\mathcal{S}$  is cold, undissociated,  $A_2$  and that its speed of flow into  $\mathcal{S}$  is hypersonic;  $\mathcal{S}$  converts the majority of the kinetic energy in the cold stream into thermal energy and, in present circumstances, it suffices to treat the flow behind  $\mathcal{S}$  as one of constant enthalpy (i.e. ignore  $\frac{1}{2}V^2$  relative to  $h$  in (8.10)). In the same spirit of providing a rough sketch rather than a detailed picture of events downstream of  $\mathcal{S}$ , assume that  $h$  is given simply by  $C_p T + cD$ , where  $C_p$  is a constant; the energy equation then reduces to the statement that

$$\Gamma T + c\vartheta_d \approx \Gamma T_b, \quad \Gamma \equiv C_p W_2/\mathbb{R}, \quad (10.4)$$

where  $T_b$  is the value of  $T$  at point B (figure 2a) since  $c$  is zero there.

Now re-arrange (10.1) together with (10.4) to give an equation for  $\vartheta$ ;

$$\vartheta \equiv T/T_b, \quad (10.5)$$

as follows:

$$d\vartheta/dt = -\epsilon \exp(1/\epsilon(1 - (1/\vartheta))) \{ [1 - \epsilon\Gamma(1 - \vartheta)] - \epsilon^2\beta_e \exp(1/\epsilon((1/\vartheta) - (1/\vartheta_e))) (\Gamma(1 - \vartheta))^2 \}, \quad (10.6)$$

where

$$\beta_e \equiv (\rho/\rho_a) \exp(1/\epsilon\vartheta_e), \quad (10.7)$$

$$\epsilon \equiv T_b/\vartheta_a, \quad (10.8)$$

$$t = \epsilon^{-2} \exp(-1/\epsilon) \int_0^{\xi_1} \left( \frac{\sigma_1 \Omega}{V\Gamma} \right) d\xi_1 \quad (10.9)$$

and  $\vartheta_e (= T_e/T_b)$  gives the final, equilibrium, values of  $\vartheta$  at which all further chemical activity ceases, calculated from the transcendental expression (cf.  $\{ \} = 0$  in (10.6))

$$1 - \epsilon\Gamma(1 - \vartheta_e) = \epsilon^2\beta_e(\Gamma(1 - \vartheta_e))^2, \quad (10.10)$$

where  $\beta_e$  will take values in the neighbourhood of unity. The various quantities, in particular  $t$  in (10.9), have been defined so as to make  $d\vartheta/dt$  equal to  $-1$  at the initial 'instant'  $t = 0$ , where  $\vartheta (= \vartheta(t; \epsilon))$ , is such that

$$\vartheta(0; \epsilon) = 1. \quad (10.11)$$

The parameter  $\epsilon$  in (10.8) is moderately small, of order  $10^{-1}$ , and the idea that was exploited by Birkhan *et al.* and derived from work in combustion theory (reviewed by Williams 1985), is to seek asymptotic solutions for  $\vartheta$  in the limit as  $\epsilon \rightarrow 0$  with, in the first instance at least,  $t$  fixed. This process is expedited by using a nonlinear coordinate transformation due to Kassoy (1975), which in the present situation can be written as

$$\lambda = \epsilon \ln(1 + t) \quad (10.12)$$

with

$$\vartheta \sim (1 + \lambda)^{-1} + \epsilon\vartheta^{(1)}(t). \quad (10.13)$$

For any  $\vartheta - \vartheta_e > O(\epsilon)$  the final, recombination, term in (10.6) is negligible and substitution of (10.12), (10.13) into (10.6) produces the result

$$\vartheta^{(1)} = -2(1 + \lambda)^{-2} \ln(1 + \lambda) \quad (10.14)$$

via the most elementary manipulations.

When  $\vartheta - \vartheta_e$  is  $O(\epsilon)$  the recombination term in (10.6) is no longer negligible; dissociation has proceeded, very rapidly at first, and then at a diminishing rate, until the atom concentration begins to approach its local equilibrium value. In such circumstances, defining  $\zeta$  via

$$\epsilon\zeta \equiv 1 + \lambda - \vartheta_e^{-1}, \quad (10.15)$$

allows one to show that

$$\vartheta^{(1)} = (1 + \lambda)^{-2} \ln \{ (1 + \lambda)^{-2} + e^\zeta \} \quad (10.16)$$

when  $\zeta = O(1)$ . In other words

$$\vartheta \sim \vartheta_e + \epsilon\vartheta_e^2 \ln(1 + \vartheta_e^2 e^{-\zeta}) \quad (10.17)$$

under these circumstances.

Figure 8 illustrates these results (in particular (10.13) combined with (10.14), and

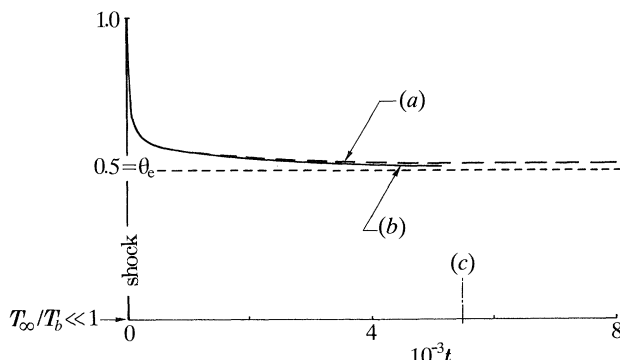


Figure 8. Temperature against coordinate  $t$  (see (10.9)) behind a strong normal shock in a dissociating gas. The final equilibrium value of  $\vartheta$  is  $\vartheta_e$  ( $=0.5$  in the present case);  $\epsilon$ , defined in (10.8), is  $10^{-1}$ . (a) Recombination included, (b) no recombination, (c)  $\vartheta_e^2 \exp\{(1/\vartheta_e - 1)/\epsilon\}$ .  $\vartheta = T/T_b$ .

(10.17)) for some typical conditions, and makes two important features of the chemical behaviour downstream of a strong shock quite clear. The first feature is the extremely rapid rate of fall of temperature as the virtually unchecked processes of dissociation take energy out of the flow to break chemical bonds; the second is the comparatively slow and spatially protracted progress towards final chemical equilibrium. Of course  $t$  is a nonlinearly stretched spatial coordinate;  $\sigma_1$  may be given a constant value without loss of generality, but  $\Omega$  and  $V$  both change in the relaxation zone behind  $\mathcal{S}$ . However, such changes are not dramatic and figure 8 can be interpreted roughly as a qualitative picture of the spatial variation of  $T$  or  $\vartheta$ .

The implicit limitation of the method, as described above, to small-order  $\epsilon$  values of  $c$  should be remarked upon. More details and numerical values for their particular example are described by Birkhan *et al.* The method should be capable of development into more complex and accurate situations than the one outlined above; certainly the acquisition of an asymptotic solution, with the usual strong links that these solutions make with essential physical behaviour, is very useful in a teaching context.

### Oblique plane waves

Although the treatment in the foregoing subsection is brief it is, hopefully, clear that a satisfactorily complete summary of the endothermic reaction domain downstream of, and normal to,  $\mathcal{S}$  is available. For the very strong waves that have been examined it has been found that  $T$  diminishes monotonically from its value at B (cf. figure 2a) to its final equilibrium value at E, whilst  $c$  increases monotonically. This has been demonstrated for the simplest reaction scheme. One thing that figure 2a suggests is that pressure  $p$  and density  $\rho$  ( $=1/v$ ) also increase monotonically in the reaction zone from B to E; since the figure applies to much more general circumstances than those of a single reaction and reactant, the conclusion about the behaviour of  $p$  and  $\rho$  is likewise more general than the previous statements about  $T$  and  $c$ .

As  $\rho$  increases in the reaction, or relaxation, region the flow velocity normal to  $\mathcal{S}$  must diminish. Addition of a fixed component of velocity that is parallel to  $\mathcal{S}$  (cf. (5.6), for example) to the whole flow pattern now provides a solution for the flow through a plane oblique shock and its associated plane reaction zone. The situation is illustrated in figure 9. The flow is instantaneously deflected through shock  $\mathcal{S}$  by

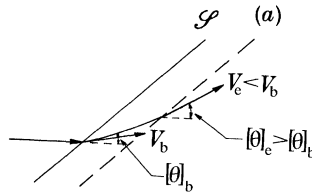


Figure 9. Streamline through a plane oblique shock-plus-reaction zone.  
(a) Effective end of the relaxation zone (cf. figure 8).

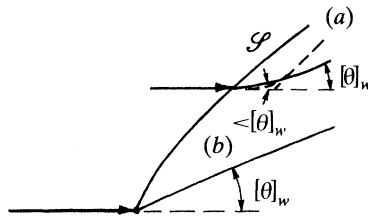


Figure 10. The effect of a simple wedge, of opening-angle  $[\theta]_w$ , on shock  $\mathcal{S}$  attached to the apex; the flow is one with finite-rate chemistry. (a) Effective end of the relaxation zone, (b) zone of vorticity created by the curved shock  $k$ , continuously, by chemical reactions.

an amount  $[\theta]_b$  and then undergoes additional deflection in the relaxation zone to reach a final value  $[\theta]_e > [\theta]_b$ .

It is possible to imagine that  $\mathcal{S}$  springs directly from a sharp concave corner in an initially flat wall, but it is quite clear that the wall angle must then change, increase in fact, in order for it to support the plane oblique wave sketched in figure 9. The actual length scale of the reaction zone depends upon factors such as  $\Omega$ ,  $V$  and  $\epsilon$ , as indicated in the previous subsection; therefore the same shape of solid body will not produce the same flow field (specifically, not a simple planar field) under different atmospheric conditions. Just as the similitude solution for continuous expansive flows does not appear in a reacting medium (cf. §7), so its compressive counterpart is of much less significance in the construction of supersonic reacting flow fields.

### Plane wedge

The plane wedge shape is a basic artefact of supersonic flows in simple ideal gases and so it is interesting to find out how a reacting flow will respond to its presence.

Assume that flow downstream of an oblique shock wave is given sufficient space to reach new states of equilibrium. With a uniform equilibrium flow ahead of the wedge the picture must be as illustrated in figure 10. The explanation for figure 10 is as follows. Far downstream of the corner the flow must be parallel with the wedge surface;  $\partial\theta/\partial\xi_1$  must vanish and (8.9) shows that  $p$  must be uniform across this whole region. The total flow deflection angle through the combination of  $\mathcal{S}$  and its relaxation zone far above the wedge must therefore be the same as the wedge angle  $[\theta]_w$ ; from figure 9 it can be seen that  $[\theta]_e$  far above the wedge must be equal to  $[\theta]_w$  and that shock  $\mathcal{S}$  out there is therefore weaker than it must be at the nose of the wedge, as a result of the inequality between  $[\theta]_e$  and  $[\theta]_b$ .

Evidently entropy  $s$  will differ from streamline to streamline and the final equilibrium state will not be one of either uniform chemical composition or flow



velocity (cf. figure 6); it will, of course, be a rotational flow. It is also clear that the streamlines will not be parallel, one to the other, in the field between shock  $\mathcal{S}$  and the new equilibrium state.

*Blunt bodies and detached shocks*

Any steady supersonic stream that blows towards a blunt body will have to pass through a more-or-less highly curved shock that stands ahead of the body, as indicated in figure 11. Evidently the shape of the body has a primary (geometrical) influence on the shape of  $\mathcal{S}$ , but one must also remember that the chemical condition of the gas between  $\mathcal{S}$  and the body will have a part to play in the shape and location of the shock, as has just been indicated in the case of the simple wedge.

There is a significant difference between the present configuration and those examined so far in this section. The only length scale that has mattered so far is the local chemical scale  $V\tau_d$  (see (10.1)), but now the body introduces a specific length scale of its own, such as the radius of curvature  $r_s$  of the body at the stagnation point S (figure 11).

The distance NS is called the shock stand-off distance. If the flow has no intrinsic length scale, NS is a fraction of  $r_s$  that depends only upon body shape and free-stream Mach number  $M_\infty$ , but for any finite, non-zero, value of  $V\tau_d$  this is no longer the case. For example, suppose that  $V\tau_d$  is so small relative to  $r_s$  everywhere in the neighbourhood of the stagnation streamline NS that, for all practical purposes, the flow along that streamline is in chemical equilibrium. As a result (cf. figure 2a) the density will be larger there than it would be in the opposite situation, for which  $V\tau_d$  is assumed to be large enough to make the flow from N to S predominantly one of fixed or frozen composition. Clearly shock stand-off distance will be smaller when equilibrium conditions prevail than in the opposite limit, for which composition is frozen.

It is interesting to observe that the frozen-flow limit of large ( $V\tau_d/r_s$ ) cannot apply uniformly along NS since  $V$  must become arbitrarily small as the stagnation point S is approached. Thus, no matter how large  $\tau_d/r_s$  may be near S its product with  $V$ , outside the singular case of  $\tau_d$  infinite, must ultimately tend to zero. It is clear from (10.1) that  $c$  must approach an equilibrium value at S under all circumstances, with the possibility that a small region of near-equilibrium composition may exist in a near neighbourhood of S, buried within a predominantly fixed-composition shock layer. This interesting and quite complex topic has been very fully treated by Conti (1966) and Conti & Van Dyke (1969a, b).

In the plane flow, pressure, density and temperature vary along streamlines in the following way:

$$(\alpha_f^2 - V^2) p_{\xi_1} = \rho V^2 \alpha_f^2 \hat{\sigma} \theta_{\xi_2} + V^2 Q c_{\xi_1}, \quad (10.18)$$

$$(\alpha_f^2 - V^2) \rho_{\xi_1} = \rho V^2 \hat{\sigma} \theta_{\xi_2} + Q c_{\xi_1} \quad (10.19)$$

$$\rho \alpha_f (\alpha_f^2 - V^2) T_{\xi_1} = (\gamma_f - 1) \hat{\sigma} \rho V^2 \theta_{\xi_2} - (1 - \gamma_f M_f^2) Q c_{\xi_1} - \gamma_f (1 - M_f^2) (\partial p / \partial c)_{\rho, T} c_{\xi_1}. \quad (10.20)$$

The notation is that of §8, with the following additions:

$$\alpha_f \equiv (1/v) (\partial v / \partial T)_{p, c_2}, \quad \hat{\sigma} \equiv \sigma_1 / \sigma_2, \quad Q \equiv (\partial e / \partial c)_{p, \rho}.$$

The ratio of frozen specific heats is written as  $\gamma_f$ ;  $\gamma_f$  is not necessarily a constant.

It can now be seen directly that changes of  $p$ ,  $\rho$  and  $T$  along streamlines occur for two fundamental reasons; one is geometric, in the sense that  $\theta_{\xi_2} \neq 0$  in general, and the other is chemical since  $c_{\xi_1}$  is likewise not usually zero.

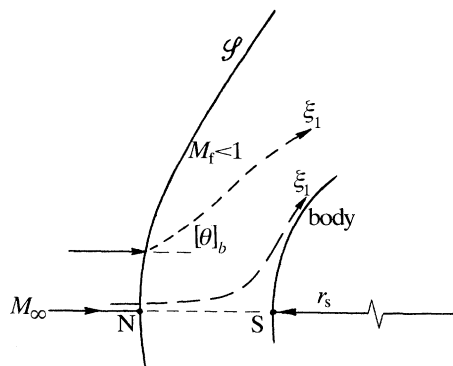


Figure 11. Flow near the stagnation point S of a symmetrical body; NS is stand-off distance shock  $\mathcal{S}$ .

The flow downstream of the nearly-normal parts of shock  $\mathcal{S}$  is subsonic, which means  $a_f^2 > V^2$  in this case; if  $\mathcal{S}$  itself is strong enough, the even stronger condition  $\gamma_f M_f^2 > 1$  will apply, and this will certainly be the case for a bow shock  $\mathcal{S}$  in a hypersonic stream. If  $\theta_{\xi_2}$  is zero it can be seen that  $T_{\xi_1}$  is negative (since  $c_{\xi_1}$  must be positive behind  $\mathcal{S}$  prior to a new state of chemical equilibrium), which reaffirms what has already been seen in the section on normal plane shock behaviour.

In regions near NS the term  $\theta_{\xi_2}$  is positive (cf. figure 11), so that the chemically-induced rates of decrease of  $T$  are checked by geometric effects as the flow is decelerated near the stagnation point. Evidently  $p$  and  $\rho$  rise monotonically along streamlines in these regions and even  $T$  will begin to increase in close proximity to S.

The magnitude of  $c_{\xi_1}$  will diminish as dissociation proceeds and, in any case, one will eventually encounter a switch in the sign of  $\theta_{\xi_2}$  as progress is made along a streamline (see figure 11). The expansive character of the flow that is clearly associated with  $\theta_{\xi_2} < 0$  (see (10.18)) means that geometric effects will now augment the fall in  $T$  that is associated with the progress of dissociation. As a result  $\tau_d$  can increase dramatically beyond what is called for by chemical action alone (cf. (10.3) and the large activation energy implicit in  $\vartheta_d$  there). For all practical purposes the chemical reactions then cease and the expansive flow proceeds, downstream of a thin 'transition' layer, in an effectively frozen condition. That all of this is not mere speculation is amply borne out by the very enterprising experimental and theoretical work carried out by Stalker & Hornung and their colleagues (reviewed recently by Hornung (1988)). Of course, whether or not the thin transition layer occurs in the relatively low-speed parts of a flow somewhere near a stagnation point depends entirely on the magnitudes of a local Damköhler number such as  $r_s/V\tau_d$ , but there is no doubt at all that it can happen.

## 11. Combustion in high-speed flow

Suppose that a plane shock  $\mathcal{S}$  exists in a stream of pre-mixed reactants whose enthalpy  $h$  obeys the elementary relation given in (6.4). A very brief account of what may happen when  $\mathcal{S}$  is normal to the unburnt cold reactant stream has already been given in §6 (cf. figure 2c), where the whole combination of shock plus reaction zone (or fast flame) has been identified as a ZND detonation wave. Detonation waves, in

which exothermic chemical reactions drive a strong shock which then acts as the ignition mechanism for the chemical activity, have long been the subject of experimental and theoretical examination, and many books, review articles and papers have been written about them. The book by Fickett & Davis (1979) is an authoritative source of information up to that date, and it is clear that most work on detonation is provoked by the need to understand how such waves propagate in gases, liquids and solids. As a result the main body of this work deals with, or at least implies, time dependence. The possibility of sustained hypersonic flight in the atmosphere depends upon the provision of a satisfactory propulsion device and, since detonations travel at supersonic speeds normal to themselves (cf. §6) and so can maintain a fixed position in a supersonic stream, it is natural to start thinking of them as essentially steady-state processes for the release of chemical energy within an engine. Flow speeds need not be matched precisely to the propagation speed of the detonation, which tends to be very closely tied to the energy released in the chemical reaction, since the wave can be oblique to the oncoming flow. The combination of high speeds of normal propagation (e.g. Mach numbers of 3–5) and obliquity make detonations natural processes for heat addition at hypersonic speeds and fundamental work on possible flow configurations was begun many years ago (e.g. Townend (1970), who first demonstrated the need for detonations to be oblique to have flexible and efficient ramjet performance).

Of course the need for a pre-mixed stream of reactant gases into which the detonation can propagate turns the emphasis firmly in the direction of mixing processes in the hypersonic environment. This crucial topic is not within the scope of this article, but it is very important to know that mixing can be satisfactorily achieved in such conditions, although fuel–air ratio may vary widely across the gas stream, as exemplified in the recent work of Menees *et al.* (1990).

There is space here for only a very brief outline of the way in which steady-state exothermic waves may behave in supersonic streams. In essence, what follows is concerned with the simple spatial structure of such waves in an attempt to bridge the distance that exists between treatments of exothermic influence in the manner of a discontinuity (e.g. a jump from O to E<sub>D</sub> in figure 2*c* (Townend 1970)) and in the manner of distributed sources of heat (cf. Broadbent, this Theme).

#### *Normal exothermic wave*

Consider the wave whose broad character is indicated in figure 2*c*, which consists of a shock-jump  $\mathcal{S}$  from O to B followed by a combustion zone B to E<sub>D</sub>. The structure of this last zone can only be determined once the nature of the relevant particular chemical reaction is known. A suitably simple source term that is both sufficient for present purposes and consistent with the naive thermodynamics implied by (6.4) is

$$K_{\alpha} = -\rho\Omega c \exp(-\vartheta_a/T), \quad (11.1)$$

where  $\Omega$  is a pre-exponential frequency factor (a weak function of  $\rho$  and  $T$ ) and  $c$  is the mass-fraction of the combustible species;  $\vartheta_a$  is an activation temperature (cf. (10.2) which defines  $\vartheta_d$  in terms of activation energy for a dissociation reaction).

Combustion is a process that is noted for its sensitivity to the levels of temperature in a system. Consistently with the simple modelling of thermodynamics and chemistry in this article it is convenient, first, to define

$$\epsilon \equiv T_b/\vartheta_a \quad (11.2)$$

and then to affirm the temperature sensitivity just referred to by making

$$\epsilon \ll 1. \quad (11.3)$$

Immediately downstream of shock  $\mathcal{S}$ , in other words from point B on the Rayleigh line  $\mathcal{L}_2$  in figure 2c, conditions develop in such a way that it is proper to write

$$\psi = \psi_b(1 + \epsilon\psi'), \quad \psi = p, \rho, V, T. \quad (11.4)$$

The domain in which perturbations of the foregoing quantities from their values at point B, denoted by  $p_b$ , etc., are limited to  $O(\epsilon)$  is described as the induction domain  $\mathcal{I}$ .

When flow-deflection angle  $\theta$  is constant (e.g. zero) (8.7)–(8.11) can be manipulated to show that

$$T'_\chi = \Gamma \exp(T'), \quad \Gamma \equiv (1 - \gamma M_b^2)/(1 - M_b^2), \quad (11.5)$$

where  $M_b (< 1)$  is the frozen Mach number of the flow at B and  $\chi$  is related to distance  $\mathbb{S}$  measured along a streamline from point B as follows:

$$\epsilon \exp(1/\epsilon)\chi = (c_b Q/C_{pf} T_b)(\Omega_b/V_b)\mathbb{S}. \quad (11.6)$$

(Note that  $\mathbb{S}$  is such that  $d\mathbb{S} = \sigma_1 d\xi_1$  in the notation of §8.) Evidently (11.5) makes

$$T' = -\ln(1 - \Gamma\chi) \quad (11.7)$$

and domain  $\mathcal{I}$  concludes with temperature rising like the logarithm of  $1 - \Gamma\chi$  in the neighbourhood of  $\chi = 1/\Gamma$  which, in company with (11.6), gives physical scale to the induction event. Only  $O(\epsilon)$  fractions of reactant are consumed in  $\mathcal{I}$ .

Thereafter the combustion process goes through a sequence of diminishing length scales as temperature increases until all of the remaining reactant is consumed. The whole situation has been discussed in some detail by Kassoy & Clarke (1985).

It will be helpful in what follows to describe the physically compact domain in which most of the reactant is consumed, and pressure falls (from just below B to  $E_D$  in figure 2c), as the fast-flame domain, or  $\mathcal{F}$  for short. More information about fast flames in the context of one-dimensional unsteady events can be found in a paper by Clarke (1989a).

For practical purposes the reaction zone, made up from  $\mathcal{I}$  and  $\mathcal{F}$ , occupies a layer whose thickness, perpendicular to  $\mathcal{S}$ , is of order

$$(V_b/\Omega_b)(C_{pf} T_b/c_b Q)\epsilon \exp(1/\epsilon)/\Gamma. \quad (11.8)$$

It is clear that this length scale can vary over a wide range of values, depending upon the size of a number of parameters, and that it is entirely possible to find the  $\mathcal{I}$  and  $\mathcal{F}$  domains comparable in size with geometrically significant parts of a propulsion device.

The particular detonation wave O to B to  $E_D$  in figure 2c is a Chapman–Jouguet (CJ) wave (Fickett & Davis 1979) since Rayleigh line  $\mathcal{L}_2$ , and hence mass-flux through the wave (equivalent to propagation speed), is fixed by the relative disposition of points O and  $E_D$  in the plane; as a result the propagation speed of a CJ detonation is determined entirely by the thermodynamics of the gas mixture and not at all by chemical rate processes. CJ detonations are the ones that usually appear in experiments on waves in tubes (Fickett & Davis 1979). It should be noted that flow-speed at  $E_D$  in such a wave is exactly (frozen, in the present case) sonic, and that CJ wave propagation speed, in the present situation, is a lower bound for all detonation speeds.

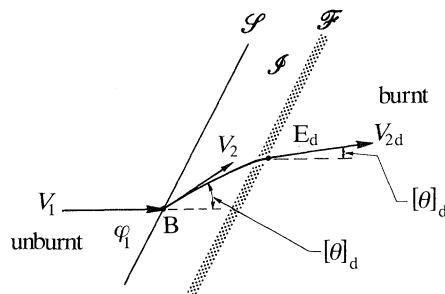


Figure 12. A plane oblique detonation wave;  $\mathcal{S}$  is the shock wave,  $\mathcal{I}$  is the (relatively long) induction domain,  $\mathcal{F}$  is the (relatively short) fast-flame. Deflection angle  $[\theta]$  diminishes monotonically from  $[\theta]_b$  to  $[\theta]_d > 0$ .

### Oblique exothermic waves

By vectorially adding a component of flow velocity that is both parallel to a wave of the kind that has just been described, and of the same magnitude throughout the field, a picture such as figure 12, can be constructed. This shows the effect of a plane oblique detonation on the local streamline pattern. It is axiomatic that the stream ahead of such a wave must be uniform in all respects.

Flow deflection  $[\theta]_b$  through  $\mathcal{S}$  at point B can be substantial, but further changes (which must be reductions) of  $\theta$  in  $\mathcal{I}$  are of order  $\epsilon$ . Thereafter, some further and substantial reductions in  $\theta$  take place through  $\mathcal{F}$  until the final increment from the pre-shock direction, namely  $[\theta]_d$ , is achieved at point  $E_D$  (figure 2c). Flow deflections must always obey the inequality

$$[\theta]_b > [\theta]_d > 0 \quad (11.9)$$

when  $\mathcal{S}$  is at a positive acute angle  $\varphi_1$  to the local stream.

With  $V_1$  ahead of  $\mathcal{S}$  well in excess of  $a_{T_1}$  it is clear that any sudden change in the direction of a solid surface through an angle  $[\theta]_b$  will create a shock  $\mathcal{S}$ , and that the jump in temperature experienced by reactant on crossing  $\mathcal{S}$  will switch on combustion reactions. However, if the surface immediately downstream of B is not shaped to conform to the streamline shape indicated in figure 12, it is evident that the combination of  $\mathcal{S}$ ,  $\mathcal{I}$  and  $\mathcal{F}$  will not be plane and the wave system therefore not CJ.

### More general combustion wave systems

Suppose that a sharp wedge W with a half-angle  $[\theta]_b$  is situated in a relatively cold uniform stream of pre-mixed reactants. The wedge angle is assumed to be small enough to admit an attached shock  $\mathcal{S}$  at the apex (figure 13), so that flow downstream of  $\mathcal{S}$  will be supersonic. Assume furthermore that, although  $\mathcal{S}$  need not be exactly plane, it is not far removed from that condition, so that the sort of ordering of perturbations in the induction-domain that was described above can be extended to the initial field downstream of  $\mathcal{S}$ . It is only necessary to write

$$\theta = \epsilon\theta' \quad (11.10)$$

in addition to (11.4) to be able to show from (8.7)–(8.11), and after a good deal of algebra, that

$$(T'_x - \Gamma e^{T'})_{xx} - (T'_x - e^{T'})_{\psi\psi} = 0, \quad (11.11)$$

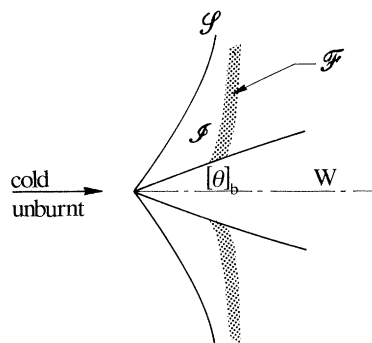


Figure 13. The effect of a symmetrical sharp wedge situated in a relatively cold high-speed stream of unburnt reactants (cf. figure 12 for notation).

where  $\Gamma$  and  $\chi$  are formally the same as in (11.5) and (11.6). The new coordinate  $\psi$  is related to the coordinate  $\mathbb{N}$  normal to streamlines via

$$\epsilon \exp(1/\epsilon) \psi = (c_b Q / C_{pf} T_b) (\Omega_b / V_b) (|M_b^2 - 1|)^{\frac{1}{2}} \mathbb{N}, \quad (11.12)$$

where  $\mathbb{N}$  is such that  $d\mathbb{N} = \sigma_2 d\xi_2$  in §8. (Compare (11.12) with (11.6).)

It should be noted that, while  $V_b$  and  $M_b$  are flow speed and Mach number at point B both here and in the sub-section on normal exothermic waves,  $M_b < 1$  in the latter situation (in fact  $\gamma_f M_b^2 < 1$  is implied in (11.7) and (11.8)) whilst  $M_b > 1$  is necessary here; the important thing is that  $\Gamma$  should be positive throughout (cf. Kassoy & Clarke (1985) for a description of ‘quenching’ of combustion activity by compressibility effects when  $\gamma_f < M_b^2 < 1$ ).

The temperature perturbation equation (11.11) is formally the same in the present two-dimensional steady supersonic flow as it is in a one-dimensional unsteady environment (Clarke 1981). As a consequence, many results and implications from studies of the latter equation (Clarke & Cant 1985; Jackson & Kapila 1985; Friedman & Herrero 1988; Blythe & Crighton 1989) can be taken over directly to the present case of exothermic steady flow.

In particular, the appearance of a locus or ‘path’ of logarithmic singularities in solutions for  $T$ , in the neighbourhood of  $\chi = \chi_s(\psi)$ , say, heralds the appearance of a strong combustion wave, that consumes all of the reactant, and is the two-dimensional steady (curved) analogue of the (straight) domain  $\mathcal{F}$  described above. So long as the radius of curvature of the locus  $\chi_s(\psi)$  is much larger than its thickness the local structure of the combustion wave at  $\chi_s(\psi)$  will be given by Hugoniot-curve–Rayleigh-line theory. The foregoing remarks draw on work by Kapila & Dold (1991) and Dold & Kapila, summarized by Clarke (1989*b*), for plane unsteady wave development.

The possibilities for the control of combustion-energy release through such mechanisms as the shaping of solid boundaries and the use of cross-stream variations in chemical composition (cf. slip surfaces  $\mathcal{C}$  in §5) are considerable. Combinations of  $\mathcal{S}$ -waves with ‘ $\mathcal{I} + \mathcal{F}$ ’ combustion domains need not be limited to the combinations that make up such things as CJ detonations. That a much wider range of possibilities for the association of shocks and fast flames exists can be inferred from both the analytical work of Kapila & Dold (1991) and the numerical studies by Clarke *et al.* (1986, 1990) and Clarke & Singh (1989) of one-dimensional unsteady situations.

More extreme situations than those that can be described in the compass of  $O(\epsilon)$  perturbations in  $\mathcal{I}$ -domains must be investigated by numerical methods. The method outlined in §8 for two-dimensional steady supersonic flows has a number of advantages when it comes to general body, body-plus-engine-intake, propulsive-duct shapes in the presence of slip surfaces, and much more complex chemistry than has been used for the illustrative/didactic purposes of the present account of the flow of high-speed reactive gases.

## References

- Anderson, J. D., Jr 1989 *Hypersonic and high temperature gas dynamics*. New York: McGraw-Hill.
- Batchelor, G. K. 1967 *An introduction to fluid dynamics*. Cambridge University Press.
- Bird, G. A. 1976 *Molecular gas dynamics*. Oxford University Press.
- Birkhan, M. A., Law, C. K. & Kassoy, D. R. 1988 Transient decomposition-recombination dynamics of dissociating and ionizing gases. *Proc. R. Soc. Lond. A* **418**, 331–343.
- Blythe, P. A. & Crighton, D. G. 1989 Shock-generated ignition: the induction zone. *Proc. R. Soc. Lond. A* **426**, 189–209.
- Chapman, S. & Cowling, T. G. 1952 *The mathematical theory of non-uniform gases*, 2nd edn. Cambridge University Press.
- Christiansen, W. H., Russel, D. A. & Herzberg, A. 1975 Flow lasers. *A. Rev. Fluid Mech.* **7**, 115–139.
- Clarke, J. F. 1969 Small-Disturbance Theories. In *Non-equilibrium flows*, Part I (ed. P. P. Wegener). New York: Marcel Dekker.
- Clarke, J. F. 1981 On the propagation of gas dynamic waves in an explosive atmosphere. *Prog. Astronaut. Aeronaut.* **76**, 383–402.
- Clarke, J. F. 1989a Fast flames, waves and detonation. *Prog. Energy Combust. Sci.* **15**, 241–271.
- Clarke, J. F. 1989b Developments in detonation theory. Keynote paper KS-10 in *Proc. 10th Aust. Fluid Mech. Conf.* Melbourne, Australia: Research Publications.
- Clarke, J. F. & Cant, R. S. 1985 Nonsteady effects in the induction domain behind a strong shock wave. *Prog. Astronaut. Aeronaut.* **95**, 142–163.
- Clarke, J. F. & McChesney, M. 1964 *The dynamics of real gases*. London: Butterworths.
- Clarke, J. F. & McChesney, M. 1976 *Dynamics of relaxing gases*. London: Butterworths.
- Clarke, J. F. & Singh, G. 1989 A numerical simulation of shock-generated ignition using the random choice method. In *Proc. Third Int. Conf. on Numerical Combustion*, Lecture Notes in Physics, vol. 351, pp. 22–35. Heidelberg: Springer-Verlag.
- Clarke, J. F., Kassoy, D. R. & Riley, N. 1986 On the direct initiation of a plane detonation wave. *Proc. R. Soc. Lond. A* **408**, 129–148.
- Clarke, J. F., Kassoy, D. R., Meharzi, N. E., Riley, R. & Vasantha, R. 1990 On the evolution of plane detonations. *Proc. R. Soc. Lond. A* **429**, 259–283.
- Conti, R. J. 1966 A theoretical study of non-equilibrium blunt-body flows. *J. Fluid Mech.* **24**, 65–88.
- Conti, R. J. & Van Dyke, M. D. 1969a Inviscid reacting flow near a stagnation point. *J. Fluid Mech.* **35**, 799–813.
- Conti, R. J. & Van Dyke, M. D. 1969b Reacting flow as an example of a boundary-layer under singular external conditions. *J. Fluid Mech.* **38**, 513–535.
- Courant, R. & Friedrichs, K. O. 1948 *Supersonic flow and shock waves*. New York: Interscience.
- Dorrance, W. H. 1962 *Viscous hypersonic flow*. New York: McGraw-Hill.
- Einstein, A. 1920 Schallausbreitung in teilweise dissoziierten Gasen. *Sitzber. Berliner Akad. Wiss.* 380–385.
- Emanuel, G. 1986 In *Gas dynamics: theory and applications*, AIAA Education Series (ed. J. S. Przemieniecki). New York: AIAA.
- Fickett, W. & Davis, W. C. 1979 *Detonation*. London: University of California Press.
- Friedmann, A. & Herrero, M. S. 1988 *IMA Preprint 462*, University of Minnesota, U.S.A.
- Phil. Trans. R. Soc. Lond. A* (1991)

- Hayes, W. D. 1960 *Gasdynamic discontinuities*, no. 3. Princeton Aeronautical Paperbacks, Princeton University Press.
- Hayes, W. D. & Probstein, R. F. 1966 *Hypersonic flow theory*, 2nd edn. New York: Academic Press.
- Hirschfelder, J. O., Curtiss, C. F. & Bird, R. B. 1954 *Molecular theory of gases and liquids*. New York: John Wiley.
- Hornung, H. 1988 Experimental real-gas hypersonics. *Aeronaut. J.* 379–389.
- Jackson, T. L. & Kapila, A. K. 1985 Shock-induced thermal runaway. *SIAM Jl appl. Math.* **45**, 130–137.
- Kapila, A. K. & Dold, J. W. 1991 In *Proc. 9th Symp. (Int.) on Detonation*. Portland, Oregon. (In the press.)
- Kasoy, D. R. 1975 Perturbation methods for mathematical models of explosion phenomena. *Q. Jl Mech. appl. Maths.* **28**, 63–74.
- Kasoy, D. R. & Clarke, J. F. 1985 Structure of a steady high-speed deflagration with a finite origin. *J. Fluid Mech.* **150**, 253–280.
- Liepmann, H. W. & Roshko, A. 1957 *Elements of gasdynamics*. New York: John Wiley.
- Lighthill, M. J. 1956 Viscosity effects in sound waves of finite amplitude. In *Surveys in mechanics* (ed. G. K. Batchelor & R. M. Davies), pp. 250–351. Cambridge University Press.
- Lighthill, M. J. 1957 Dynamics of dissociating gases, Part I. *J. Fluid Mech.* **2**, 1–32.
- Menees, G. P., Adelman, H. G. & Cambier, J. L. 1990 Analytical and experimental investigations of the oblique-detonation-wave engine concept. In *Proc. AGARD PEP, 75th Symp.* Madrid.
- Mughal, M. S. 1989 Hypersonic flow of a vibrationally-relaxing gas past a slightly-blunted wedge. Ph.D. thesis, Cranfield Institute of Technology, U.K.
- Park, C. 1990 *Nonequilibrium hypersonic aerothermodynamics*. New York: Wiley-Interscience.
- Strang, G. 1968 On the construction and comparison of finite-difference schemes. *SIAM J. numer. Analysis* **5**, 506–517.
- Thompson, P. A. & Lambrakis, K. C. 1973 Negative shock waves. *J. Fluid Mech.* **60**, 187–208.
- Toro, E. F. 1989 A weighted-average flux method for hyperbolic conservation laws. *Proc. R. Soc. Lond. A* **423**, 401–423.
- Townend, L. H. 1970 Detonation Ramjets for Hypersonic Aircraft. *RAE Tech. rept.* 70218.
- Vincenti, W. G. & Kruger, C. H. 1965 *Introduction to Physical Gas Dynamics*. New York: John Wiley.
- Wegener, P. P. 1969 *Nonequilibrium flows*, Part I. New York: Marcel Dekker.
- Wegener, P. P. 1970 *Nonequilibrium flows*, Part II. New York: Marcel Dekker.
- Whitham, G. B. 1963 The Navier–Stokes Equations of Motion. In *Laminar boundary layers* (ed. L. Rosenhead), ch. III. Oxford: Clarendon Press.
- Whitham, G. B. 1974 *Linear and Nonlinear Waves*. New York: Wiley-Interscience.
- Williams, F. A. 1985 *Combustion Theory*, 2nd edn. Menlo Park, California: Benjamin/Cummings.
- Zel'dovich, Ya. B. & Raizer, Yu. P. 1966 *Physics of shock waves and high-temperature hydrodynamic phenomena*, vols 1 & 2. New York: Academic Press.